PREPARATION OF FERRITE LAYERS BY ELECTROPHORETIC DEPOSITION

HEE AY CHING

FACULTY OF ENGINEERING

UNIVERSITY OF MALAYA

KUALA LUMPUR

2012

PREPARATION OF FERRITE LAYERS BY ELECTROPHORETIC DEPOSITION

HEE AY CHING

DISSERTATION SUBMITTED IN FULFILMENT OF THE REQUIREMENTS FOR THE DEGREE OF MASTER OF ENGINEERING SCIENCE

FACULTY OF ENGINEERING

UNIVERSITY OF MALAYA

KUALA LUMPUR

2012

UNIVERSITY MALAYA

ORIGINAL LITERARY WORK DECLARATION

Name of Candidate: HEE AY CHING

Registration/Matric No: KGA090005

Name of Degree: Master of Engineering Science

Title of Project Paper/ Research Report/ Dissertation/ Thesis ("This Work"):

Preparation of Ferrite Layers by Electrophoretic Deposition

Field of Study: Ceramic Materials

I do solemnly and sincerely declare that:

(1) I am the sole author/writer of this Work;
(2) This work is original;
(3) Any use of any work in which copyright exists was done by way of fair dealing and for permitted purpose and any excerpt from, or reference to or reproduction of any copyright work has been disclose expressly and sufficiently and the title of the Work and its authorship have been acknowledge in this Work;
(4) I do not have any actual knowledge nor do I ought reasonably to know that the making of this work constitutes an infringement of any copyright work;
(5) I hereby assign all and every rights in the copyright to this work to the University of Malaya (UM), who henceforth shall be owner of the copyright in this work and that any written consent of UM having been first had and obtained;
(6) I am fully aware that if in the course of making this work I have infringed any copyright whether intentionally or otherwise, I am be subject to legal action or any other action as may be determined by UM.

Candidate's Signature Date

Subscribed and solemnly declared before,

Witness's Signature Date

Name:
Designation:

ABSTRAK

Ferit nikel zink dan ferit magnesium tembaga zink dengan saiz zarah purata sebanyak 22.7 nm dan 26.6 nm masing-masing telah disintesiskan melalui teknik microemulsions air dalam minyak. Nilai koersivitas bagi ferit magnesium tembaga zink dan ferit nikel zink ialah 126 Oe dan 25.5 Oe masing-masing, menunjukkan kelakuan feromagnet lembut. Satu ampaian berkoloid yang mengandungi serbuk ferit yang halus disebarkan dalam etanol disediakan dengan menggunakan Phosphate Ester (PE) sebagai agen pengecas bersama-sama dengan Poly Vinyl Butyral-co-vinyl-alcohol-co-vinyl (PVB) dan Poly Ethylene Imine (PEI) sebagai penjilid dan penyelerak masing-masing. Kesan penggunaan PE terhadap kestabilan ampaian ferit telah dipertingkatkan dengan menganalisa perhubungan pH, kekonduksian dan potensi zeta ampaian tersebut. Proses pengenapan elektrophoretik (EPD) dilakukan dengan menggunakan ampaian ferit yang paling stabil. Voltan yang diaplikasikan, jenis bahan elektrod, jarak pemisahan elektrod dan konsentrasi serbuk dalam ampaian ferit dikenal pasti untuk mendapatkan lapisan ferit yang berkualiti tinggi. Mikrograf elektron pengimbasan pancaran medan bagi ferit nikel zink dan ferit magnesium tembaga zink melapiskan filem homogen dalam bentuk jarum struktur hablur. Belauan sinar-x dan tenaga spektroskopi x-ray sebar mengesahkan komposisi lapisan enapan ferit. Mikroskop daya atom dan mikroskop daya magnet membezakan antara magnetik dan fasa-fasa yang tidak magnetik bagi lapisan enapan ferit.

ABSTRACT

Nickel zinc ferrite and magnesium copper zinc ferrite powders with average particle size about 22.7 nm and 26.6 nm respectively were synthesized by water-in-oil microemulsion technique. The coercivity values for magnesium copper zinc ferrite and nickel zinc ferrite were 126 Oe and 25.5 Oe respectively which indicates soft ferromagnetic behaviour. A colloidal suspension of the fine ferrite powder in ethanol was prepared. Phosphate Ester (PE) was added to the suspension as charging agent, Poly Vinyl Butyral-co-vinyl-alcohol-co-vinyl acetate (PVB) as binder and Poly Ethylene Imine (PEI) as dispersant. The effect of the charging agent on the stability of the ferrite suspension was improved by analyzing the pH, conductivity and zeta potential of the suspension. EPD process was carried out from the most stable ferrite suspension. The applied voltage, the types of electrode materials, the electrode separation distance and the concentration of the powder in the suspension were investigated in order to obtain high quality ferrite layers. Field emission scanning electron micrographs for both sintered nickel zinc ferrite and magnesium copper zinc ferrite layers exhibit a homogeneous film composed of needle-like crystal structure. X-ray diffraction and energy dispersive x-ray spectroscopy confirmed the composition of the ferrite layers formed. Atomic force microscope and magnetic force microscope have been employed to differentiate between magnetic and non magnetic phases in ferrite layers.

ACKNOWLEDGEMENT

With the deepest gratitude I wish to thank my beloved supervisor, Dr. Henk Metselaar for providing a define guidance and intellectual support. Dr Henk is willing to spend his time to teach and explain to me whenever I encountered problems. Without his encouragement, I would not be able to excel my projects successfully.

Secondly, I would like to acknowledge and express my gratitude to the laboratory assistants, Mr. Said and Mr. Zaman who has assisted me on using the equipments in laboratory. Never forgetting to thank my workmates, Azadeh and Hakimeh for giving me invaluable suggestions and share some experiences with me.

I acknowledge financial support from Science Fund (03-01-03-SF0515), Ministry of Science, Technology and Innovation Malaysia and Postgraduate Research Grant (PS096/2009B), Institute of Research Management and Consultancy (IPPP).

Last but not least, I wish to express my appreciation to everyone who has come into my life and inspired, touched, and illuminated me through their presence. I have learned something from all of you to make my graduate studies valuable as well as enjoyable. Thank you.

TABLE OF CONTENTS

CHAPTER 5 CONCLUSION AND RECOMMENDATIONS

LIST OF FIGURES

LIST OF TABLES

LIST OF ABBREVIATIONS

AFM	Atomic Force Microscope
AGM	Alternating Gradient Magnetometer
AOT	Sodium Dioctylsulfosuccinate
CRT	Cathode Ray Tubes
CSD	Chemical Solution Deposition
CVD	Chemical Vapor Depostion
EDX	Energy Dispersive X-ray Spectroscopy
EMC	Electromagnetic Compatibility
EPD	Electrophoretic Deposition
FE-SEM	Field Emission Scanning Electron Microscope
ICDD	International Centre for Diffraction Data
IEP	Isoelectric Point
MFM	Magnetic Force Microscope
PE	Phosphate Ester
PEI	Polyethyleneimine
PVB	Poly (vinyl butyral-co-vinyl-alcohol-co-vinyl acetate)
PVD	Physical Vapor Deposition
SPM	Scanning Probe Microscope
TEM	Transmission Electron Microscope
TGA	Thermogravimetry Analysis
VP	Variable Pressure
XRD	X-ray Diffraction

LIST OF SYMBOLS

A	Area
C	Particle mass concentration
ε_0	Permittivity of vacuum
ε_r	Relative permittivity
E	Electric field
H^+	Hydronium ion
M	Molar
Mw	Molecular weight
η	Viscosity
O^-	Oxygen ion
pH	Potentiometric hydrogen ion concentration
t	Deposition time
μ	Electrophoretic mobility
μl	Microliter
V	Volt
ω	Deposit yield
W	Water to surfactant ratio
wt%	Weight percent
ζ	Zeta potential

CHAPTER 1

INTRODUCTION

1.1 Background

Ferrite thin films exhibit a slew of frequencies ranging from 1 MHz to 200+ MHz and have great potential in the design of miniaturization of magnetic devices such as micro-inductors and micro-transformers (Hashi *et al*, 2004). New communication systems require magnetic devices using microwave integrated circuits with incorporated thin ferrite films (Ravinder *et al*, 2003). These films are suitably fabricated by electrophoretic deposition (EPD), a processing technique for production of novel inorganic nanostucture such as forming densely packed ceramic films from particulate precursors. EPD is highly compatible with different combinations of materials and it is cost effective and requires only a simple setup (Boccaccini *et al*, 2006). The cost and processing time are greatly reduced with the ease of deposition of controlled thickness multilayer films on substrates of complex shape (Mehrali *et al*, 2011).

Today, there is a great demand to fabricate soft nanomagnetic materials and its associated devices for electronic and telecommunications devices. Current inductive components in a semiconducting chip are the major impediment for miniaturization of electronics, as conventional microsized magnetic materials can only be used at very low frequencies, *e.g.*, high permeability bulk ferrites can only be used at less than 1 MHz frequencies, and bulk Ni-ferrites, although they can be used up to 100 MHz, have a low permeability of only ~12. Thus, current commercial efficient converters are still designed to be operated with frequency range in less than 2 MHz.

For nanograined materials, the soft magnetic properties originate from the exchange coupling of the neighboring magnetic nanoparticles results in the intergrain interactions. This interaction tends to average the anisotropy of each individual particle, leading to higher permeability (Kurinec *et al*, 2006), reduced loss, thus possibly being used for required higher device operation frequencies.

Future economically viable miniaturized high frequency electronic components require a low loss high frequency magnetic nanocomposite that is compatible with the silicon wafer processing technology. By using a new magnetic nanocomposite thin film that can be deposited onto silicon wafers with reasonable cost, such as the electrophoresis technique reported in this work, it is possible to reduce the embedded inductor in size and increase its inductance (Raj *et al*, 2005).

EPD takes place when the charged particles dispersed in a suitable suspension move towards an oppositely charged electrode under an applied electric field. Deposition is achieved via particle coagulation. In electrostatic stabilization, these particles which must repel each other to be stably suspended become attached to each other by Van der Waals attraction or chemical bonding, forming a solid deposit (Hashi *et al*, 2004). Electrophoretic motion of charged particles in the suspension during EPD leads to the accumulation of particles and subsequently formation of a homogeneous rigid deposit on a substrate.

To effectively apply EPD technique in materials processing, it is pivotal to have a stable suspension with suitable solvent and additives (Zhitomirsky, 2000). The charged particles suspended in the liquid must be in directional motion when an electric field is applied. Stability of suspension and the directional motion are influenced by the zeta potential of the charged particles and pH of the suspension. Hence, EPD can be applied to almost any fine powder with particle size <~30 μm or as a colloidal suspension, including metals, polymers and ceramics.

The zeta potential is crucial in stabilizing the suspension by determining the intensity of repulsive interaction of particles as well as the direction and velocity of particle migration. It can be manipulated by the addition of charging agents (acids, bases, polyelectrolytes) to the suspension. Hence, there exist a wide range of additives that influence the magnitude and polarity of charge (Zarbov *et al*, 2004). Adherence and strength of the deposit can be improved by addition of binders (Doungdaw *et al*, 2005). In general, a heat-treatment method is required after deposition to further densify the deposit and to eliminate porosity. Suitable sintering conditions are also necessary in order to obtain ceramic films with desired properties (Kuscer *et al*, 2010).

In this study, water-in-oil microemulsion technique was used to prepare fine and uniform ferrite powders. A colloidal suspension of fine ferrite powder in ethanol was prepared using Phosphate Ester (PE) as the charging agent with Poly Vinyl Butyral-co-vinyl-alcohol-co-vinyl acetate (PVB) and Poly Ethylene Imine (PEI) as binder and dispersant respectively. PE is an effective electrostatic stabilizer which

positively charges the particles by donating electrons to the surface of the particles so that they can move towards the cathode. The effect of the amount of PE on the stability of the suspension was investigated by analyzing the pH, conductivity and the zeta potential of the suspension. The effect of solid concentration by varying the weight percentage of ferrite powder in the suspension was studied. The effects of applied voltage, types of electrode materials and electrodes separation distance on the thickness of deposition were determined. The surface morphology and composition of the deposited ferrite layers were later characterized by Field Emission Scanning Electron Microscope (FE-SEM), Energy Dispersive X-ray Spectroscopy (EDX), X-ray diffractometer (XRD), Atomic Force Microscope (AFM) and Magnetic Force Microscope (MFM).

1.2 Scope of Research

The aim of this study is to produce a thin and dense ferrite layer by means of EPD. A key step in producing a controlled thin layer is by suitable manipulation of zeta potential, pH, conductivity, viscosity and solid concentration of the suspension.

The ferrites with the composition of $Ni_{0.5}Zn_{0.5}Fe_2O_4$ and $Mg_{0.09}Cu_{0.34}Zn_{0.57}Fe_2O_4$ were selected for this research because they are reported to possess optimum all-round properties among other ferrites composition. Soft ferrite films are gaining its interest in the design of high frequency devices. This is due to their large electrical resistivity and high permeability. However, ferrite films are not often employed for these devices, because of the high temperature substrates or post-deposition heat treatment

requirements to obtain the micrometer range, dense films with spinel structure. EPD is found to be the solution for these specific requirements to deposit thin ferrite films (Hashi et al, 2006).

In the present work, water-in-oil microemulsion technique is used to produce finer-grained ferrites particles. Phosphate Ester (PE) is used as the charging agent to determine the stability of suspension. PE is an effective electrostatic stabilizer which creates partial positive charges on the surface by donating electrons to the surface of the particles so that they can move towards the cathode. The use of PE in non-aqueous solvents offers several advantages for EPD processing. Phosphate ester serves as a steric dispersant by anchoring the long chain molecules to the particle surfaces (Zhitomirsky, 2000).

Deposition parameters are studied in order to produce a crack-free, dense and smooth ferrite thin film. These manipulations of parameters include the solid concentration in the suspension, types of electrode, voltage variation and electrode separation distance.

A detailed study of the correlation between pH and zeta potential of the suspension system is conducted. Using standardized parameters for EPD, the deposition from the most stable suspension was characterized by FE-SEM. Microstructure and composition of the ferrite layers formed was characterized by XRD and EDX. Surface metrology of the ferrite film was carried out using AFM and MFM.

1.3 Objectives

The primary objectives of this research are:

i. To prepare ferrite powders by water-in-oil microemulsion method and identification of particle size as well as magnetic properties of the ferrite nanoparticles.

ii. To determine the solvent and additives for a well-stabilized suspension.

iii. To manipulate electrophoretic deposition parameters such as the types of electrode, voltage applied and electrode separation distances to obtain a dense homogeneous deposition.

iv. To prepare ferrite layers on a substrate by means of electrophoretic deposition (EPD) at room temperature.

v. To characterize the deposited ferrite layers on the substrate with suitable equipments such as FE-SEM, EDX, XRD, AFM and MFM.

CHAPTER 2

LITERATURE REVIEW

2.1 Background

Electrophoretic deposition (EPD) is a widely used technique to make coatings and thin films and has gained world-wide attention for a variety of applications such as automotive, appliance and general industrial (organic) coatings. Key attributes to a desirable deposition depend on the suspension stability and several other parameters.

EPD is discovered by the renowned Russian scientist – Ruess in 1808. It was first practically applied in 1933 to deposit Thoria particles on a platinum cathode as an emitter for electron tube applications. Since then, EPD demonstrated promising potential in fabrication of unique microstructures and nanostructures as well as novel and complex materials combinations in various macroscopic shapes, dimensions and orientations. At present, EPD has been greatly utilized in the processing of functional and composite ceramics, thin films, high performance ceramic, and also to produce advanced nanostructured materials.

There are several advantages of the electrophoretic deposition over the conventional dipped or sprayed coatings, some of which are high adherence and high density of the electrophoretically deposited coating, homogeneous deposits with high microstructural uniformity and low levels of pollution. EPD provides suitable control of deposit thickness and subsequently deposits coatings on a wide range 3D complex and porous structures (Corni *et al*, 2008). A simple experimental setup is required for EPD

thus renders a low cost and high efficiency fabrication method.

2.2 Ferrite

The general composition of ferrite is $MeFe_2O_4$, where “Me” represent one or more divalent transition metals (Mn, Zn, Ni, Co, Cu, Fe, or Mg). Ferrites are commonly known to be rigid, hard and brittle materials which are chemically inert. The colours appear to be in a range from silver gray to black (Ong, 2007). Specifically for $Ni_{0.5}Zn_{0.5}Fe_2O_4$ and $Mg_{0.09}Cu_{0.34}Zn_{0.57}Fe_2O_4$, they are dark brownish. This Ni-Zn ferrite and Mg-Cu-Zn ferrite are classified as soft ferrite and theoretically possess several advantages over other ferrites like the Ni-Cu-Zn ferrite due to their high compositional variability (Burrieaci *et al*, 1977).

2.2.1 Structure and Properties of Ferrite

The ferrite which contains nickel and zinc was found to form homogenously at lower temperatures and given well controlled properties (Zahi *et al*, 2007). The strong preference for the tetrahedral and octahedral sites in nickel and zinc respectively, make nickel ferrite a model inverse ferrite and zinc ferrite a model normal ferrite. Nevertheless, mixed spinel structure is found in the composite Ni-Zn ferrites. Properties of these ferrites can be modified due to compositional variation in the redistribution of metal ions over the tetrahedral and octahedral sites (Shahane *et al*, 2009).

The $Mg_{0.09}Cu_{0.34}Zn_{0.57}Fe_2O_4$ used is highly subjected to its elemental composition and physical configuration. The copper content enhances the permeability factor due to

a larger grain size and lowers the resistivity of the compound. Magnesium increases the initial permeability, however, an excess of magnesium elevates the sintering temperature. Presence of zinc increases the magnetic moment and initial permeability of the compound (Koay, 2004). Hence, low magnesium, moderate copper and high zinc contents offer optimal all-round properties of ferrite.

There are two common types of ferrite: hard ferrite and soft ferrite. Hard ferrites exhibit permanent magnetism characteristics while soft ferrites are ferrimagnetic with low coercivity. Figure 2.1 displays the hysteresis loop of soft and hard magnetic materials. Ni-Zn ferrite and Mg-Cu-Zn ferrite in particular are classified as a soft ferrite with low hysteresis loss and coercive force (Callister, 2003). Therefore, a relatively smaller, thinner and narrow area within the hysteresis loop is observed for soft ferrites.

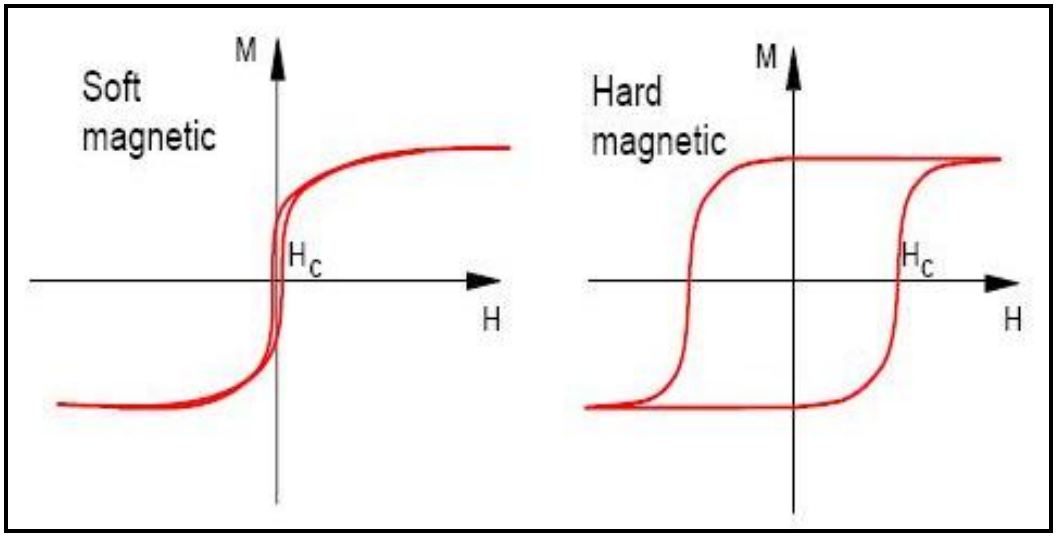

Figure 2.1: Hysteresis loop of soft and hard magnetic materials.

Soft magnetic ferrites are a class of materials which possess spinel structure, with a general formula of AB_2O_4. It is generally cubic, with the O^- ions forming a FCC lattice.

The cations (usually metals) which have 32 O^- ions in the unit cell with total of 8 octants occupy 1/8 of the tetrahedral sites (A site) and 1/2 of the octahedral sites (B site).

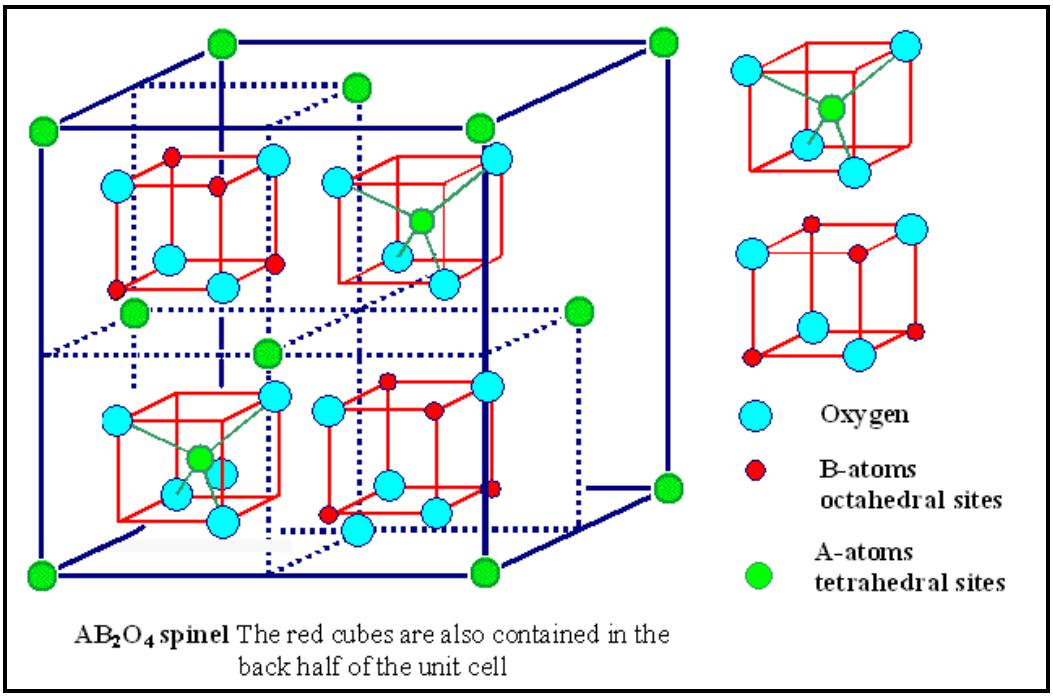

Figure 2.2: The spinel structure (Internet Reference, 7/9/2009a).

As shown in Figure 2.2, A sites are usually occupied by divalent metal ions (Mn^{2+}, Zn^{2+}, Ni^{2+}, Co^{2+}, Cu^{2+}, Fe^{2+}, or Mg^{2+}). A complete spinel structure has a unit cell of eight FCC lattices of which formed by 64 tetrahedral sites and 16 octahedral sites (Internet Reference, 7/9/2009b).

2.2.2 Applications of Ferrite

For four decades ferrite components have been employed in various applications and in steadily increasing quantities. This section discusses briefly some application of ferrites in common domestic and industrial applications, which are summarized as follows (Sahara, 1969):

(a) Ferrite Cores

In the 1950s, the introduction of television (TV) in large scale was a major opportunity for bringing up the ferrite industry. In TV sets, ferrite cores were the material of choice for the picture tube deflection system and high voltage transformer. The combination of low core cost and low core losses making ferrite an ideal core material for inverters, inductors and transformers in the frequency range 5 kHz to 100 kHz. At present, Mn-Zn ferrite is denoted as the mainstream industrial product of core materials. The Mn-Zn ferrite is usually classified into three purposes based on the basis of its properties: inductors and telecommunications parts for low-loss materials; wide-band and pulse transformer for high initial permeability; and power applications for high-saturation magnetization.

(b) Microwave Ferrites

Ferrite materials have been employed in many microwave devices, such as various types of circulators, isolators, magnetostatic resonators, filter, switches, limiters, and tunable electro-optic modulators. The most often used microwave ferrites include the bulk and film yttrium iron garnet (YIG), lithium ferrites, spinel- type Ni-Zn, Mn-Mg-Zn

and hexagonal-type barium ferrites. Presently, the exponential growth in microwave communication though mobile and satellite communications has further emphasized the importance of microwave devices using ferrite materials, due to the extremely low-loss and low cost.

(c) Ferrite Wave Absorber

A ferrite wave absorber has gaining worldwide attention in response to an increasing demand of a counter-plan for electromagnetic compatibility (EMC). This ferrite absorber can be expected to decay, for instance, forged echoes in ships' radar signals, television ghosting and electromagnetic wave leakage from various electric equipments. Ferrite plate backed with a conductive metal plate is the typical electromagnetic wave absorber. The materials used for ferrite wave absorbers include Cu-Zn, Mn-Zn, Ni-Zn, and other substituted soft ferrites.

(d) Multilayer Ferrite Chip Inductors

A tendency to miniaturize electronic components began in the 1990s. At the same time, progress also took place in surface-mount technology. Attempts have been made to establish high-density incorporation of ferrite inductors into a printed circuit board. Accordingly, this has allowed various types of multi-layer ferrite chip inductors, with a length of 10 mm and a width of 0.5 mm, to be used in television receivers, headphone stereos, video equipment, cordless telephones, personal computers, hard disk drive systems, automobile parts, etc. At present, the most popular material used in the multi-layer ferrite chip inductors is NiCuZn ferrite.

(e) Sensors

Ferrites can be used to detect proximity, rotation, and temperature. For example, altering the position of a moveable ferrite component may change the magnetic circuit (by changing the variable air gap). Hence, proximity can be denoted by monitoring the inductance in a LC circuit. The closing of water-tight doors on ships is detected using this type of application. Similarly, rotational changes can be accomplished with displacement being circular rather than linear.

Ferrites can also be used in determining when a certain temperature has been reached. Although the actual temperature is not measured in a ferrite device, it can sense a maximum predetermined temperature for purpose of control, safety, or equipment protection. Such devices are used in heaters, motors, electric irons, soldering irons, and so forth.

2.3 Synthesis of Ferrite by Water-in-oil Microemulsion Method

New synthesis methods that are competent in molecular-level control of particle characteristics are gaining its significance in the growing scientific and technology. As such, the microheterogeneous nature of microemulsion media offers attractive possibilities, as already demonstrated for a wide range of materials, including metals, chalcogenides, metal halides, carbonates, oxides and organic polymer (Arriagada and Osseo, 1999). Water-in-oil microemulsion is one promising preparation method for the formation of very fine and uniform nanoparticles which able to achieve chemical

homogeneity (Ang, 2007). Moreover, the synthetic process involves inexpensive and less toxic iron salts and a reduced amount of organic solvent making it an economical and environmentally friendly (Daliya, 2007). Water-in-oil microemulsion is optically transparent, isotropic and thermodynamically stable. Its working principle is based on nano-sized water droplets dispersed in an oil medium and stabilized by surfactant molecules accumulated at the water/oil interface. The water to surfactant ratio controls the size of resultant particles as it controls the size of water pools within which aqueous chemical syntheses take place (Rivas, 1993). As the reactants from two microemulsions come in contact with each other due to the collision and coalescence of the droplets, a precursor or ceramic particle will be formed (Liu *et al*, 1998).

The droplets in mixing of the two microemulsions solution, one containing a salt or a complex of the metal and the other containing a reducing agent, are subject to Brownian motion due to their small size. Dimmers and other aggregates will form when they collide continuously. These aggregates are short-lived and rapidly disintegrate into droplets of the original size. The content of the water pools of the two microemulsions will divide into two halves and reaction will occur in the droplets as a result of the continuous coalescence and decoalescence process. Inorganic particles in the same size ranges as the water droplets of the starting microemulsions will eventually form. The particles can be maintained as a fine suspension for a long time. A wide range of materials including metals, metal salt and metal oxides had been prepared using this simple procedure (Holmberg, 2004). The nanoparticles are usually amorphous. However, Pileni has shown that crystalline nanoparticles can be obtained in proper choice of

conditions. Particularly, an anionic surfactant with a counterion, Me^{+} or Me^{2+}, being the cation of the metal, Me, are generated in the reaction (Pileni, 1993). The starting droplets usually contain a dilute solution of a salt and the solid particles formed are of the same size order as the starting aqueous droplets. As a result, a relatively small amount of particles, probably surrounded by water and stabilized by surfactant, and a higher amount of "empty" droplets, i.e. water droplets free of salt or inorganic particles exist in the final reaction mixture. Besides, these water droplets will be stabilized by the surfactant. Hence, in colloidal chemistry nomenclature water-in-oil microemulsion containing different salts in the water pools is transferred into a complex system in which the water pools are more or less salt free (Holmberg, 2004). The process is clearly illustrated in Figure 2.3.

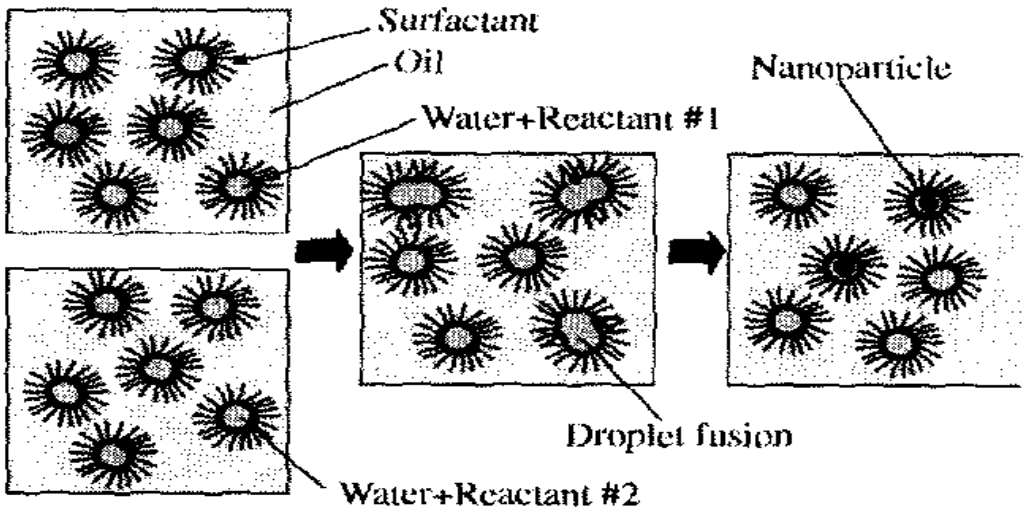

Figure 2.3: Preparation of suspended nanoparticles by mixing two water-in-oil microemulsions (Holmberg, 2004).

2.4 Electrophoretic Deposition (EPD)

Electrophoretic deposition (EPD) is a forming process in which particulate precursors are consolidated. It holds several advantages:

- Short formation time
- Requires simple apparatus
- Little restriction of the shape of substrate
- Low cost methodology
- Low temperature process
- Very versatile since it can be modified easily for a specific application

The charge on the particle and the electrophoretic mobility of the particles in the solvent under the influence of an applied electric field are two main factors for EPD process (Besra *et al*, 2007). When a DC electric field is applied, charged powder particles, dispersed or suspended in a liquid medium are attracted and deposited onto a conductive substrate of opposite charge (Corni *et al*, 2008). When the particles are positively charged, the deposition takes place on the cathode and the process is called cathodic electrophoretic deposition. Conversely, the deposition of negatively charged particles on positive electrode (anode) is termed as anodic electrophoretic deposition (Besra *et al*, 2007).

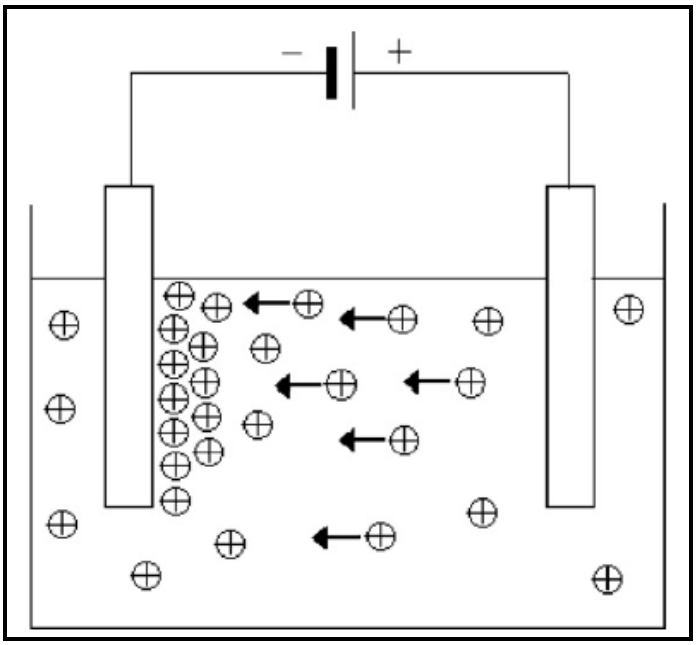

Figure 2.4: Simple two electrode cell for cathodic EPD (Corni et al, 2008).

Figure 2.4 shows the setup of a typical EPD cell. It consists of a chamber of colloidal solution and two electrodes. EPD process basically consists of two parts; first, which is the electrophoresis process, particles suspended in a liquid are forced to move toward an electrode by applying an electric field to the suspension. Initially, these particles repel each other in order to be stably suspended in the fluid. When an electric field is applied, this migration causes the particles to accumulate at the oppositely charged electrode (Hashi *et al*, 2004). Deposition, which is in the second part, the particles collect on one of the electrodes and form a coherent deposit. These particles become attached to each other by Van der Waals attraction or chemical bonding, forming a relatively compact and homogeneous film.

It is essential to obtain a stable suspension containing charged particles free to move when an electric field is applied. Similarly charged particles and similar

solvent–binder–dispersant systems are important for gaining better control of layer thickness (Besra *et al*, 2007). In general, a heat-treatment method is required after deposition to further densify the deposit and also to eliminate porosity (Corni *et al*, 2008).

2.4.1 Kinetics of Electrophoretic Deposition

The process of EPD was first described mathematically by Hamaker. The Hamaker equation correlates the amount of particles deposited (deposit yield, ω) to be directly proportional to the electrophoretic mobility (μ), the electric field (E), the electrode area (A), the particle mass concentration in the suspension (C) and the deposition time (t):

$$\omega = \mu\, E\, A\, C\, t. \tag{1}$$

The electrophoretic mobility (μ) of the particles, suspended in low-dielectric solvents, is related to the zeta potential of the particle (ζ), the solvent viscosity (η), relative permittivity of the solvent (ε_r) and the permittivity of vacuum (ε_0) of the suspension through the Hückel equation (2):

$$\mu = \frac{2\varepsilon_r \varepsilon_0 \zeta}{3\eta} \tag{2}$$

The deposition yield, as stated by the Hamaker equation, is written as

$$\omega = \frac{2\varepsilon_r \varepsilon_0 \zeta EACt}{3\eta} \tag{3}$$

Thus, deposition yield (and film thickness) can be controlled via EPD process parameters such as the electric field (E), the particle concentration (C) and the deposition time (t) (Hamaker, 1940).

2.4.2 Applications of Electrophoretic Deposition

EPD has a great potential as a low cost high volume technique for making unique microstructures and complex material combinations in a wide range of dimensions and morphologies. New applications of EPD include the low-cost fabrication of composite materials such as advanced coatings, nano-composites, laminate structures, functionally graded materials and fiber reinforced ceramics. There is also a great potential for advances in the use of EPD for piezoelectric devices, biomedical ultrasound probes, solid oxide fuel cells, chemical and biological sensors.

An insulating coating of alumina onto tungsten filaments was one of the first EPD coating applications. Thin film coatings are generally employed to protect or passivate a surface, enhance or diminish chemical reactivity, alter the conductivity or resistivity of a surface, provide higher mechanical durability and resist thermal stresses. EPD of powder phosphors typically with 0.5 – 10 μm in diameter is used in the manufacturing of cathode ray tubes (CRT) displays, exceptionally high-resolution screens (Sasaki *et al*, 1999 and Talbot *et al*, 2004). Combination of photolithography and EPD techniques have been used to fabricate colour phosphor screens (Kurinec *et al*, 1996). Recently, on-chip inductors were fabricated using EPD coating of Mn-Zn ferrites in conjunction with electrolytic plating and chemical mechanical planarization (CMP) of copper (Washburn *et al*, 2005). Nevertheless, for high frequency (~GHz) applications, NiZn ferrite is more preferable because of its superior magnetic properties at high frequencies.

2.4.3 Comparison of Electrophoretic Deposition and Laser Ablation Deposition

Thin film deposition technologies can be classified into two general methods: physical vapor deposition (PVD) and chemical deposition techniques, which include chemical vapor deposition (CVD) and chemical solution deposition (CSD). Laser ablation deposition is one of the PVD processes that uses a high power focused pulsed laser beam to ablate targets of materials to be deposited to form a deposited thin film on the substrate inside a vacuum chamber. In this technique, material is vaporized and ejected from the surface of a target as it irradiated by a laser beam. Films are formed by condensing the material ablated from the target onto a solid substrate. Absorption characteristics of the material to be evaporated determine the laser wavelength to be used. To obtain the high power density required in many cases, pulsed laser beams are generally employed. Pulse width, repetition rate, and pulse intensity are selected for specific applications.

Laser ablation deposition allows for careful control of film thickness and orientation and compatibility with the semiconductor integrated circuit processing. The main disadvantages of using this technique are the difficulty in controlling the stoichiometry of multicomponent films, the need for high temperature post deposition crystallization annealing and the high cost related with equipment acquisition and maintenance (Hassan *et al*, 2007).

Electrophoretic deposition is a wet-chemical technique that is widely used to deposit nanocomposite films. In this process, electrophoretic coating is based on deposition of a film from a dispersion of colloidal particles onto a conductive substrate. Electrophoretic deposition method allows higher deposition rates, good stoichiometry control and the production of large area defect-free films. Furthermore, lower equipment related costs incurred for film fabrication using electrophoretic deposition.

2.5 Parameters Related to Suspension System

Preparing a suitable stable suspension of particles is the first step in EPD process. This suspension must be stable from the time it is prepared until the deposit is formed. There are several criteria in selecting a suitable suspension system for deposition of powder metals via EPD. For instance are the surface properties of the powder, the influence of the type and concentration of the additives and the physicochemical nature of both suspended particle and the liquid medium (Besra *et al*, 2007). The colloidal suspension serves as a medium of charge transfer for movement of particles and providing a stable reaction without influencing the deposition on the electrode (Corni *et al*, 2008).

2.5.1 Suspension Stability

The achievement of stabilized, unagglomerated and uniform slurry is the basic ingredients in most of the colloidal processing methods of ceramic forming such as EPD. Colloidal suspensions can be prepared in the dispersed, weakly flocculated or strongly flocculated states through careful control of the inter-particle forces.

A distinct aspect of all colloidal system is that the contact area between the particle surface and the dispersing liquid is large. As a consequence, suspension behaviour is very much influenced by the surface forces. The colloidal stability is governed by the total inter-particle potential energy. Particles dispersed in the suspending medium must exhibit sufficient repulsive forces to offset the van der Waals attraction in order to get a well-stabilized suspension.

The dominating inter-particle forces in most ceramic system are:

(i) the van der Waals attractive force,

(ii) double layer (electrostatic) repulsive force, and

(iii) stearic (polymeric) forces

EPD is the event of motion of particles in a colloidal solution or suspension in an applied potential field. The process commonly takes place when the distance over which the double layer charge falls to zero is large, compared to the particle size. As such, the particles will migrate relative to the liquid phase when the electric potential is applied. Generally, a suspension whose absolute value of its zeta potential is high (>25 mV) will tend to be stable. Since the zeta potential can alternatively be described as a measure of the repulsive forces exerted by particles in a liquid medium, it follows that suspensions with a high zeta potential will likely be fairly stable.

The stability of a suspension is characterized by sedimentation rate of particles in the colloidal suspension and its probability to undergo flocculation. Stable suspensions settle slowly, show no tendency to flocculate at the bottom of the container. It will form dense and strongly adhering deposits. On the contrary, flocculating suspensions settle rapidly and form low density, weakly adhering deposits. Deposition using an unstable suspension is not likely to occur without agitation of the suspension.

However, if the suspension is too stable, deposition will not occur due to the repulsive forces between the particles will not be overcome by the electric field. According to some models for electrophoretic deposition, the suspension should be unstable when the distance of electrodes is too close with each other. This local instability could be caused by the formation of ions from electrolysis or discharge of the particles which results in flocculation of ions close to the electrode surface (Besra *et al*, 2007).

2.5.2 Particle Size

It is essential for the particulate precursor to remain completely dispersed and stably suspended in the liquid for homogeneous and smooth deposition. Although there is no general thumb rule to specify particle sizes suitable for electrophoretic deposition, good deposition for most of the ceramic and clay systems have been reported to occur in the range of 1–20 μm (Besra *et al*, 2007). Hence, EPD can be applied to any solid that is available as a fine powder with particle size of less than or equal to 30 μm. EPD is also applicable to any solid such as metals, polymers, ceramics and glasses in the colloidal

suspension (Corni *et al*, 2008).

Yet this does not necessarily mean that deposition of particles outside this particle size range is not workable. Colloidal particles with 1 μm or less in diameter tend to remain in suspension for long periods due to Brownian motion (Besra *et al*, 2007). Continuous hydrodynamic agitation is required for particles larger than 1 μm to remain in suspension. Larger particles tend to settle due to gravity. Ideally, the mobility of particles due to electrophoresis must be greater than that due to gravity. It is difficult to get uniform deposition from sedimenting suspension of large particles.

Electrophoretic deposition from settling suspension will result in a gradient in the deposition film, i.e., thinner above and thicker deposit at the bottom when the deposition electrode is placed vertical. Either a very strong surface charge must be obtained or the electrical double layer region must increase in size in order for electrophoretic deposition to occur with larger particles (Besra *et al*, 2007).

Particle size has also been found to have a large influence on controlling the cracking of the deposit during drying. Reduction in particle size improved the morphology of the film prepared by electrophoretic deposition. Thus, it is essential to reduce the particle size during EPD in order to minimize cracking of deposits (Sato *et al*, 2001).

2.5.3 Dielectric Constant of Liquid

The ideal properties in the suspension medium are low viscosity (≤ 5 cP), low conductivity (~30 μs/cm) and high dielectric constant (sometimes called the relative permittivity). This number fluctuates depending on the pH of the suspension (Besra *et al*, 2007). The dielectric constant expresses the dissociating power of the solvent (Van der Biest *et al*, 1999). Investigations evaluating deposit formation as a function of the dielectric constant (of the pure liquid) and the conductivity of the suspension have revealed that conductivity increases sharply with the dielectric constant (Powers, 1975). It has been found that a solvent with too low a dielectric constant will prohibit deposition because of insufficient dissociative power. Contrarily, a liquid medium with a high dielectric constant may reduce the size of the double layer region surrounding a particle due to the high ionic concentration in the liquid. Since particles move as a result of the distortion of the double layer, it is essential that this region be large enough to facilitate this action in a manner that results in deposit formation. Hence, a low ionic concentration is favorable in the EPD process. Finding a balance between the two extremes, expressed above, is significant to the solvent selection process.

Van der Biest and Vandeperre have suggested that aqueous suspension is beneficial for EPD process due to its low environmental cost (Van der Biest, 1999). However, there are some disadvantages using aqueous suspension such as the evolution of hydrogen bubbles and blister formation. Palladium readily absorbs hydrogen, yet the use of an aqueous system is restricted to palladium because it is expensive and cannot

be feasible for industrial use.

In general, non-aqueous organic liquids are favorable to water (aqueous) as a suspension medium for electrophoretic forming. While the generally lower dielectric constant in organic liquids limits the charge on the particles as a result of the lower dissociating power. Higher field strengths can be applied to overcome the problems of joule heating, electrolytic gas evolution and electrochemical attack of the electrodes. In addition, the organic liquids are preferred because of their good chemical stability, higher density and low conductivity. Organic solvents with a high dielectric constant like ethanol, propanol and butanol are the most suitable media for EPD (Besra *et al*, 2007). By using appropriate non-aqueous solvents, substances that are insoluble in water can be dissolved, substances that are unstable in water remain stable, and electrochemical reactions that are impossible in water become possible.

2.5.4 Conductivity of Suspension

Suspension conductivity is a critical parameter to the EPD technique. If the conductivity of a suspension is too high, the motion of the particles in solution is too slow for deposition to occur. A highly resistive suspension also prohibits deposit formation because the particles will charge electronically and become destabilized. There are pros and cons to the effect of suspension conductivity on deposit formation. For instance, it has been reported that high-conductivity suspensions yield uniform deposits, while low conductivity suspensions result in non-uniform deposits (Stappers *et al*, 2008). The likely reason for this incidence is that slow particle motion (as experienced in highly

conductive suspensions) yields a homogenous formation due to the low velocity of the particles, which prevents agglomeration; hence, the particles have more time to “order” themselves in smooth, uniform manner. It has been shown that suspension conductivity increases with temperature and dispersion concentration. Studies have also proven that there exists a somewhat tight range of conductivities over which electrophoretic deposition of materials is possible. Naturally, adjustment of other system parameters can broaden the typical range of accepted conductivities for this process (Besra *et al*, 2007). It is worthwhile to note that studies have also been published illustrating an apparent dependence of suspension conductivity on the size of the nanoparticle in the fluid (Jang *et al*, 2004).

2.5.5 Viscosity of Suspension

A suspension whose resistance to flow is weak is desirable in the EPD of nanomaterials. Since the solid loading using in the EPD technique is low, there is very little information in the literature containing a quantitative analysis of the relationship between viscosity and the state of a suspension (whether it is stable or unstable). Specifically, the total amount of nanoparticles in conventional electrophoretic deposition suspensions is not sufficiently high enough to influence the viscosity of the fluid medium (or the solvent). However, as stated above, a highly viscous liquid medium is nearly akin to an electrically resistive medium.

2.5.6 Zeta Potential

The zeta potential of particles is an important parameter in the EPD process. It plays a crucial role in the stabilization of the suspension by determining the magnitude and direction of the migration of particles during EPD, and the morphology of the deposit (Zarbov, 2004).

Theoretically, electric potential in the interfacial double layer at the location of the slipping plane versus a point in the bulk fluid away from the interface is termed as zeta potential. It is a measure of the potential difference between the particle surface and the shear layer plane formed by the adsorbed ions. As it is closely related to the particle's double layer thickness, thus it provides information on the agglomeration of the particles in the suspension. The higher the absolute value of the measured zeta potential, the better is the dispersion of the particles in the suspension (Besra *et al*, 2007).

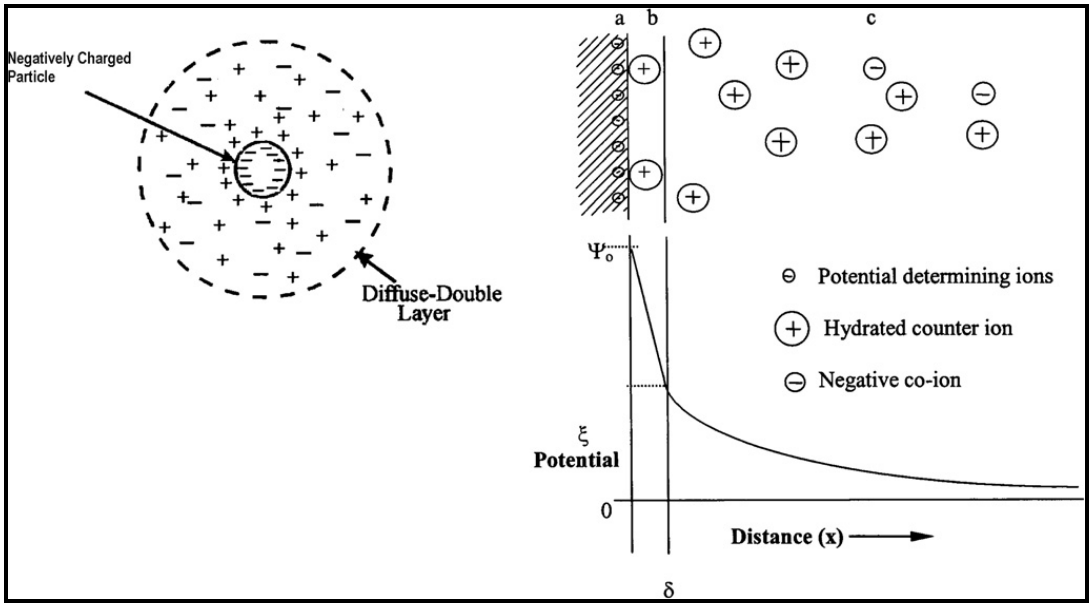

Figure 2.5: Illustration of the double layer and potential drop across the double layer (a) surface charge, (b) Stern layer, (c) diffuse layers of counter-ions (Weise, 1985).

The electrical double layer surrounding particles suspended in a colloidal solution is partially defined by the zeta potential. This double layer can be considered to consist of two parts: (1) an inner region, which includes oppositely-charged ions bound relatively strongly to the particle surface, and (2) an outer region, which is a diffuse region where the ion concentration is slightly lower than the inner region, but higher than that of the bulk fluid.

The interaction between individual particles in the suspension determines the overall stability of a system. Two mechanisms that affect this relationship are electrostatic and van der Waals forces. The probability of coagulation of a disperse system relies upon the interaction energy resulting from these two forces.

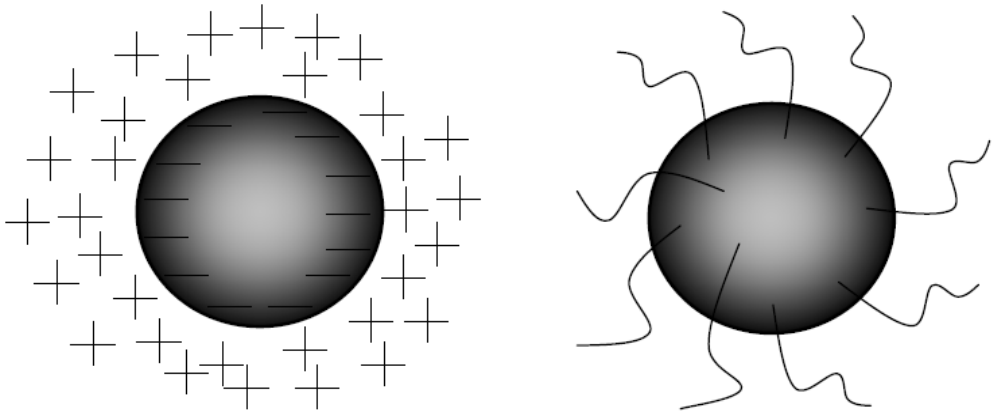

(a) (b)

Figure 2.6: Schematic illustration of (a) electrostatic stabilization, and (b) steric stabilization of particles in suspension.

A high electrostatic repulsion due to high particle charge is needed to avoid particle agglomeration. The green density of the deposit is affected by the particle charge. The particles become closer to each other and with increasing attraction force during formation of the deposit. The particles would coagulate even for relative large inter-particle distances if the particle charge is low. It will in terms lead to porous, sponge-like and non-uniform deposits.

Contrarily, the particles will repulse each other if they have a high surface charge during deposition. Thus, they will occupy positions which will lead to high particle packing density. Therefore, it is very essential to control the solids loading and concentration of solvents and additives in the EPD suspension in order to achieve the highest possible green density of the deposit. Furthermore, an assessment of the zeta potential of a suspension is of fundamental importance to the EPD technique, since it determines which electrode should be designated as the anode (+) or the cathode (-).

The zeta potential can be manipulated by a variety of charging agents such as acids, bases and specifically adsorbed ions or polyelectrolytes in the suspension. Hence, there exists a variety of additives that alter the charge magnitude and its polarity. These additives act by different mechanisms. The preferred polarity and deposition rate of the particles are the two main criteria for selection of a charging agent (Besra *et al*, 2007).

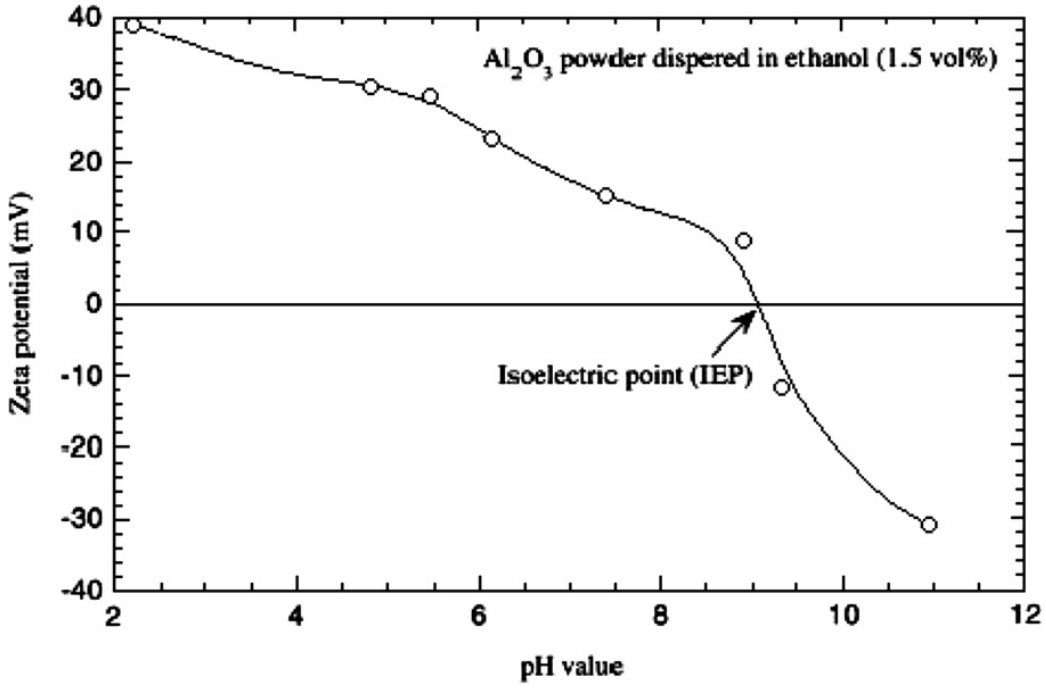

Figure 2.7: Zeta potential of Al_2O_3 powder in ethanol (Chen *et al*, 1999).

As shown in Figure 2.7, the stability and deposition rates of powder particulate from its suspension in ethanol were at maximum of which the positive zeta potential of particulate was at maximum. However, the suspensions were less stable under higher pH values. This is explained based on a charging mechanism on the particulate surface.

Under basic conditions such as pH ~11, AlOH tends to form AlO^-. Yet the presence of water is prone to bring the above reaction towards the formation of $AlOH_2^+$, rather than the formation of AlO^-. It results in an absolute value of the zeta potential greater at pH ~2 than at pH ~11. Hence, stability of suspension is higher at lower pH than at higher pH conditions (Chen *et al*, 1999).

2.5.7 Charging Agents & pH Variation

It is important that the colloidal particles in a solvent should be electrostatically stabilized for EPD process. Charge on the particles and the electrophoretic mobility under the influence of an applied potential are the driving force for EPD. These charges are usually provided by a class of additives known as the charging agents. Depending on the mode of EPD: either cathodic or anodic EPD, the charge supplied determines the direction of migration of the particulate precursors towards oppositely charged electrodes. At the same time, suitable charging agents are chosen as such not to have further chemical reaction with the particulate precursors and the excess can be easily disposed off during sintering.

Phosphate Ester (PE) as Charging Agent

Phosphate Ester (PE), or chemically known as Butyl Acid Phosphate ($(C_4H_9O)_nP(O)(OH)_{3-n}$, n=1, 2) is an effective electrostatic stabilizer which positively charges the particles in organic solvents. It donates electrons to the surface of the particle and thus promotes cationic EPD process. In the industry, PE is widely used as dispersant in the tape casting technology.

This specific type of PE is a mixture of mono and di-esters, whereby they dissociate in an organic solvent. The powder surface is positively charged when the protons (or hydronium ions) liberated from PE adsorb onto the powder. The conductivity and operational pH is a function of amount of charging agent. In cationic EPD, as the amount of charging agent increased, more hydronium ions are available in the

suspension. Hence, the pH dropped and the electrical conductivity increased.

However, when the amount of PE present is increased, the amount of adsorbed protons becomes gradually saturated and the dissociation of PE reaches the equilibrium state. Therefore, the dissociation of PE stops and excess PE molecules exist in the neutral state in the suspension (Doungdaw *et al*, 2005).

2.5.8 Effect of Polymer Binders

Polymer binders are common additives in ceramic processing. Only seldom or minimal amount of binder is utilized in the EPD processing. The role of binders in EPD processing is multifunctional. Polymer binders are used to prevent cracks and obtain adherent deposits. In addition, the adsorbed polymer can reduce viscosity of the suspension and provide stearic stabilization of suspension of ceramic particles.

In EPD processing, the polymer binder is included in the deposit due to charged polymer particles transport adsorbed polymer to the electrode surface. This is in contrast to some other ceramic techniques, where the entire dissolved polymer is included in the green body after solvent evaporation.

Therefore, the control of polymer adsorption is a crucial step in EPD. Polymer concentration in suspension and specific polymer–particle, polymer–solvent, particle–solvent and particle–dispersant interactions are the factors influencing polymer adsorption deficiency. Good solvents are indispensable in order to attain high polymer

concentration in solution. Nevertheless, the polymer can be adsorbed on the surface of ceramic particles when its solubility in the dispersion medium is low. Adsorption of polymer on ceramic particles in poor solvent will lead to bridging flocculation (Besra *et al*, 2007).

PVB as binder and PEI as dispersant

Poly (vinyl butyral-co-vinyl alcohol-co-vinyl acetate) (PVB) with an average Mw of 50,000-80,000 is commonly used as binder while Polyethyleneimine (PEI) is used as a dispersant in an organic solvent (Doungdaw *et al*, 2005).

PVB is a resin normally used for applications that require strong binding, optical clarity, adhesion to many surfaces, toughness and flexibility. It is prepared from the reaction between polyvinyl alcohol and butyraldehyde. Laminated safety glass for automobile windshields, anticorrosive coatings, and ceramic binders are the major application (Internet Reference, 9/10/2009a).

Polyethylene imine (PEI) is a highly branched aliphatic polyamine with the repeating chemical unit denoted as $–(CH_2–CH_2–NH)–$. The amine groups in PEI exist in primary, secondary and tertiary form in the approximate ratio 1:2:1. The chain terminating units which consist of primary amine groups are the most basic and reactive. Under acidic and neutral pH conditions, PEI with an average Mw of 10,000 is very effective for neutralization of excess anionic colloidal charge. Modified PEI copolymers having relatively high molecular mass can be effective for drainage and pitch control.

Pure PEI is an ideal choice for treatment of highly anionic furnish, furnish that has a high electrical conductivity, or thick-stock furnish, due to their branched nature and exceptionally high charge (Internet Reference, 9/10/2009b). PEI is soluble in most polar materials including water and alcohols.

2.5.9 Concentration of Solids

The concentration of solids in the suspension during EPD affects the morphology of the deposit. Suspensions with a large enough volume fraction of solids to form a deposit without negatively influencing its stability are ideal. In multi-component EPD systems, the optimization of the particle density in solution is of particular significance. If the particle species involved have differing surface charges, they may have conflicting deposition rates. In general, if the volume fraction of solids is high, the powders will deposit at an equal rate (Besra et al, 2007). In heterogeneous suspensions where the concentration of solids is low, the particles may deposit at rates proportional to their individual electrophoretic mobility (Vandeperre et al, 1997).

2.6 Parameters Related to Electrophoresis and Deposition

Electrophoretic deposition is a wet process which can be made on flat, cylindrical or any other shaped substrate with only minimal change in electrode design and positioning. The thickness and morphology of a deposited film can be controlled easily through simple adjustment of the EPD parameters such as the deposition time and applied potential.

2.6.1 Electrode Properties & Conductivity

The selection of electrodes is crucial as some materials can react with the suspension and destroy the process of deposition. Some electrode materials can cause gas formation and result in blisters in the deposit. Featured requirements of electrodes to be used in electrophoretic deposition are corrosion resistance, non-polluting, inertness, deformation-free and can be able to withstand a certain amount of voltage without further decomposition (Internet Reference, 2/10/2009).

However, if the electrical properties of the electrode are not ideal, particle adhesion can be relatively weak. This may lead to cracking in the film's morphology as the particles tend to struggle to "order" themselves on the surface of the electrode. If an electrode of low conductivity (i.e., a highly resistive substrate) is used during electrophoretic deposition, the deposited film will tend to be cracked and non-uniform. Stainless steel plates have thermal conductivity of 10-30 W/m-K, electronegativity of 1.86 in the Pauling Scale and melting temperature of 1538 °C. On the other hand, copper plates have thermal conductivity of 385 W/m-K, electronegativity of 1.90 in the Pauling Scale and melting temperature of 1083 °C (Callister, 2003).

It is crucial to note the melting temperatures of the electrodes as deposits on the electrodes are required to be sintered at significantly high temperatures (Doungdaw *et al*, 2005). The sintering temperature for Ni-Zn ferrite is found to be at 1400 °C (Verma, 2006). As for Mg-Cu-Zn ferrite, the sintering temperatures are found to be at 500 °C and 925 °C (Ng, 2008). Electrodes used should be able to withstand from oxidation

during this high temperature thermal processing.

2.6.2 Electrode Separation Distance

The deposition process can be facilitated by the decrease of the electrode separation distance. The tendency of particles to receive electronic charge at a distance nearer to the electrode increases, thus render the deposition rate to increase as well.

When the electrode separation distance is decreased, the current density however increased due to the increase of the conductance. It is well known that conductance is proportional to the conductor cross-section and inversely proportional to the conductor length under a uniform conductive medium. Since current density is proportional to the applied potential, a higher potential is appropriate for better deposition.

In contrast, the appropriate separation distance does not necessarily produce the best deposition. It is found that a close proximity of electrodes result in an inferior film quality and it was difficult to deposit an entire layer of film (Guo *et al*, 2000).

2.6.3 Applied Voltage

Theoretically, the accumulated ions at the electrodes restrict subsequent deposition. However, the number of free ions is generally small in organic suspensions such as in ethanol. As the voltage is increased, the accumulation of ions is no longer negligible as it greatly influences the motion of particles around the electrode. The divergence in deposition rate at different voltages is caused by the variation of particle concentration

near the electrode (Ciou *et al*, 2007).

The amount of deposit achieved during EPD generally increases with applied voltage. Although deposit formation can occur more rapidly when greater voltage is applied, the quality of the film will deteriorate. Attest to the fact that the formation of particulate film on the electrode is a kinetic phenomenon, the accumulation rate of materials influences their packing characteristics in coating (Besra *et al*, 2007).

Films deposited under the influence of a high applied field tend to be less homogeneous than films developed under lower potentials. This is because turbulence environment created at a higher applied field. Thereby disturb the coating by flows in the surrounding medium, even during its deposition. Moreover, particles in the suspension may move at a high enough velocity to coagulate on the surface of the electrode resulting in an undesirable structure (Besra *et al*, 2007).

EPD of particles influenced by too low a potential can also be detrimental to the formation of the film on the electrode. If the ions bordering a particle's electrical double layer are not supplied with enough current to facilitate electrophoresis, distortion of this layer does not occur. As such, upon the deposition phase of EPD, the particulate matter will not interact with the electrode forcefully enough to adhere to its surface. It is worthwhile to note that in some cases the properties of the solvent can also hinder the necessary distortion of a particle's double layer, which may result in poor deposit formation (or no deposit being formed at all).

2.6.4 Deposition Time

The amount of time an EPD experiment is allowed to proceed is an essential factor. It is a critical parameter that generally has a direct effect on the morphology of the deposit. Ogata, N. et al., have found that deposition rate with a fixed applied voltage decreases with increased deposition time (Ogata *et al*, 2001). Initially, during the deposition phase of EPD, there is a wealth of unoccupied sites on the surface of an electrode. As time passes, more particles aggregate on the electrode's surface, which results in an increasingly diminishing surface area available to particles for deposition. Furthermore, this layer of aggregated particles will in many instances act like an insulator, prohibiting any further film formation. In general, however, the thickness of a deposit via EPD tends to increase with deposition time. Although the rate of deposition eventually "levels out" with increasing deposition time, in most schemes, deposit formation will increase (at varying rates) until it reaches the maximum for that particular system (Ogata *et al*, 2001).

Figure 2.8 shows the deposition characteristics of hydroxyapatite at different applied potentials, with increasing deposition time. As the potential difference between the electrodes is maintained constant, the electric field influencing electrophoresis decreases with deposition time. This is largely due to the formation of an insulating layer of ceramic particles on the electrode surface. There is generally a linear relationship between deposition mass and time during the initial period of EPD (Besra et al, 2007).

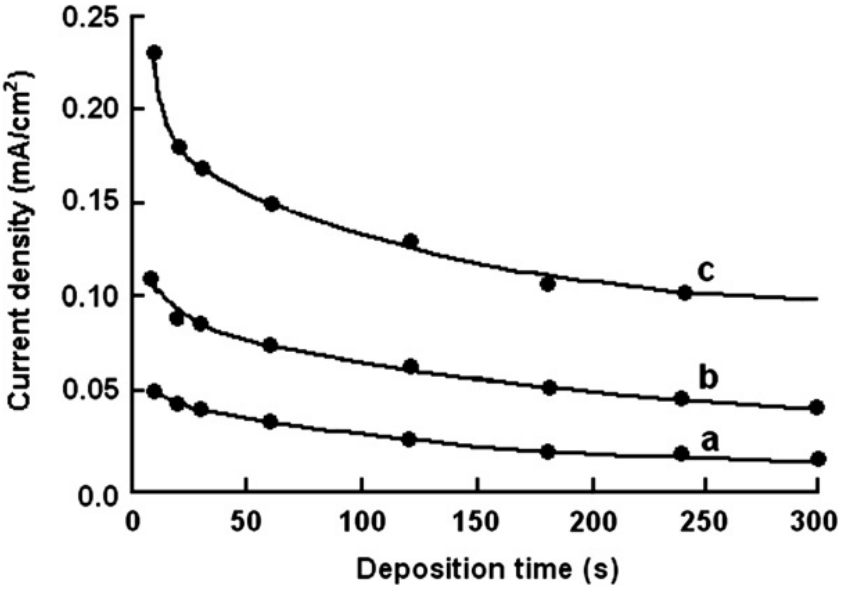

Figure 2.8: Current density versus deposition time for deposition of hydroxyapatite at different applied voltages: (a) 50 V; (b) 100 V; (c) 200 V (Besra *et al*, 2007).

2.7 Sintering

Sintering is the process of getting a dense body by heating a compacted powder for a certain time at a temperature high enough to significantly promote diffusion. However, the sintering temperature must be lower than the melting point of the main component. The purposes of the sintering process are;

1. To complete the interdiffusion of the component metal ions into the desired crystal lattice.
2. To establish the appropriate valencies for the multi-valent ions by proper oxygen control.
3. To develop the microstructure most appropriate for the application.

CHAPTER 3

METHODOLOGY

The experiments carried out for this thesis can be broadly categorized into four sections:

a. Preparation of nano powder (Ni-Zn ferrite and Mg-Cu-Zn ferrite)

b. Suspension preparation

c. EPD experiment

d. Materials Characterization

The ferrites with the composition of $Ni_{0.5}Zn_{0.5}Fe_2O_4$ (nickel zinc ferrite) and $Mg_{0.09}Cu_{0.34}Zn_{0.57}Fe_2O_4$ (magnesium copper zinc ferrite) were selected for this research because they are reported to possess optimum all-round properties among other ferrites composition. The ferrite powders in this project were synthesized by water-in-oil microemulsion process. Reverse micelle solution was prepared by combining sodium dioctylsulfosuccinate (AOT) and 2,2,4-trimethylpentane (isooctane) oil phase.

A suspension of ethanol with charging agent, dispersant and binder was prepared. The optimal concentration of suspension was determined which consisted of Phosphate Ester (PE) as the charging agent together with Poly Vinyl Butyral-co-vinyl-alcohol-co-vinyl acetate (PVB) and Poly Ethylene Imine (PEI) as binder and dispersant respectively. Conductivity, pH and zeta potential of the suspensions were measured. The effect of solid concentration by varying the weight percentage of ferrite powder in the suspension was studied.

Standard parameters for EPD like the voltage, electrode separation distance and electrode materials were employed. Electrodes of copper and stainless steel plates of dimension 25 mm x 10 mm for cathode and 25 mm x 20 mm for anode were prepared. Deposited samples were later characterized by means of Field Emission Scanning Electron Microscope (FE-SEM), Energy Dispersive X-ray Spectroscopy (EDX), X-ray Diffraction (XRD), Atomic Force Microscope (AFM) and Magnetic Force Microscope (MFM).

Specific description of each stage of methodology is shown thoroughly in this chapter. The following figure shows the overall work flow of this research.

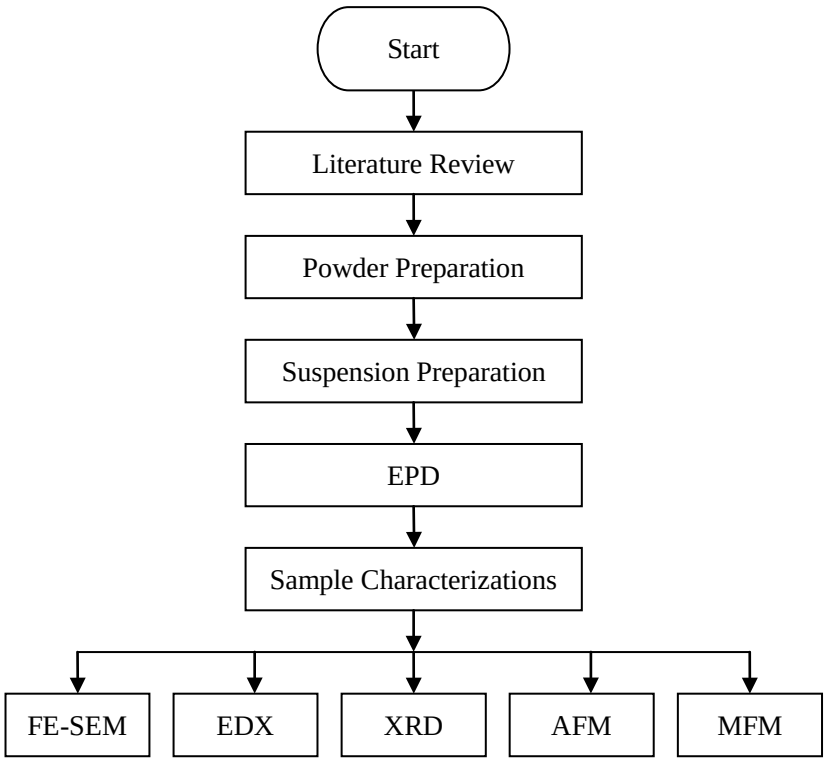

Figure 3.1: An overview of research work flow.

3.1 Preparation of Nano powder

Table 3.1: The quantity of materials required in preparing Ni-Zn ferrite powder

No.	Materials	Quantity
1.	Sodium dioctyl sulfosuccinate (AOT)	44.8 g
2.	2,2,4-trimethylpentane (isooctane)	186 ml
3.	$FeCl_2.4H_2O$	0.0887 g
4.	$NiCl_2.6H_2O$	0.0475 g
5.	$ZnCl_2$	0.0273 g
6.	NH_4OH	1 ml
7.	methanol	200 ml

Table 3.2: The quantity of materials required in preparing Mg-Cu-Zn ferrite powder

No.	Materials	Quantity
1.	Sodium dioctyl sulfosuccinate (AOT)	44.8 g
2.	2,2,4-trimethylpentane (isooctane)	186 ml
3.	$FeCl_2.4H_2O$	0.0887 g
4.	$MgCl_2.6H_2O$	0.0203 g
5.	$CuCl_2.2H_2O$	0.0511 g
6.	$ZnCl_2$	0.0273 g
7.	NH_4OH	1 ml
8	Methanol	200 ml

A reverse micelle solution was prepared first by combining 0.56 M of sodium dioctylsulfosuccinate (AOT) (R&M Chemicals, UK) with a 2,2,4-trimethylpentane (isooctane) (Merck kGaA) oil phase. The reverse micelle solution was then divided into two halves. 0.07 M $FeCl_2.4H_2O$ (Strem Chemicals, USA), 0.02 M $NiCl_2.6H_2O$ (R&M Chemicals, UK) and 0.02 M $ZnCl_2$ (R&M Chemicals, UK) were mixed to make an aqueous metal solution. The water to surfactant ratio (*w*) was fixed at 15.5 with the relative volume of AOT solution to water as 6:1. The first half of the reverse micelle solution was added volumetrically to the aqueous metal solution. An analogous solution that had been made using water and concentrated ammonia in a 1:1 ratio was added to the second half of the reverse micelle solution. Both the reverse micelle solutions containing metal aqueous solution and ammonia solution were agitated until each one was visibly clear and transparent. The reverse micelle containing metal solution was placed in an addition funnel and added to the reverse micelle solution containing ammonia under constant stirring, allowing the reacting species to come in contact with each other due to the dynamic nature of the dispersed droplets. The product microemulsion turned to green colour initially, after which the solution turned yellowish under constant stirring over a period of a few minutes. The mixture was stirred vigorously for two hours to complete the reaction. Excess methanol was added to the resulting mixture to disrupt the micelles and to desorb the surfactant molecules from the particles. Two layers solution appeared immediately after adding methanol to the reverse micelle solution showing oily form for the upper layer and colourless for bottom part of the solution. The resulting product was collected by a centrifuge and washed repeatedly with methanol until all AOT was removed. Following that, the colloidal

precipitate was dried in a vacuum chamber for 24 hours.

In a typical experimental procedure, magnesium copper zinc ferrite nanoparticles were prepared by dissolving 0.07 M $FeCl_2.4H_2O$ (Strem Chemicals, USA), 0.01 M $MgCl_2.6H_2O$ (Ajax Finechem, Australia), 0.03 M $CuCl_2.2H_2O$ (Fisher Chemicals, Malaysia) and 0.02 M $ZnCl_2$ (R&M Chemicals, UK) as the aqueous phase in the reverse micelle solution. Water to surfactant ratio (*w*) was maintained at 15.5. Ammonia solution is added to the second half reverse micelle solution. The two obtained solutions were mixed and stirred vigorously for two hours. Methanol is added and the mixture was then centrifuged. Brown fine powder $Mg_{0.09}Cu_{0.34}Zn_{0.57}Fe_2O_4$ (magnesium copper zinc ferrite) was obtained.

Mettler TGA/SDTA851e Thermogravimetry Analysis (TGA) was performed to determine the calcination temperature of the ferrite samples. Structural characterization of the ferrites was carried out using Philips PW 3040 X-Ray Diffractometer (XRD) and LEO-Libra 120 Transmission Electron Microscope (TEM). Magnetic property of the ferrites was characterized by MicroMag^{TM} 2900 Alternating Gradient Magnetometer (AGM) from the Princeton Measurement Corporation. The ferrite powders were then ready to be used in the proceeding EPD processes.

3.2 Suspension Preparation

For the purpose of EPD, suspensions were prepared by dispersing the ferrite particles in ethanol solvent. Phosphate Ester (PE) was selected as it is reported to provide better control in suspension stability and superior properties as a charging agent (Doungdaw *et al*, 2005). High molecular weight polymer, Poly Vinyl Butyral-co-vinyl-alcohol-co-vinyl acetate (PVB) was added into the non-aqueous suspension as binder material to promote structural stability and strength of the deposit. Poly Ethylene Imine (PEI) was added as dispersant to promote stabilization of ferrite particles in the colloidal suspension.

3.2.1 Percentage of Charging Agent

The zeta potential of the surfaces of nanoparticles in colloidal suspensions is a key factor in evaluating the stability of dispersions used in EPD. In order to study the variation of zeta potential, conductivity and pH of the suspension, the amount of charging agent was manipulated. It is necessary that a low, dilute concentration of particles be used in order to achieve the quality EPD of materials. A solid loading of 1 wt% was used as the particle concentration to eliminate settling during the measurement process. Suspensions with 99 wt% ethanol solvent, 1 wt% of ferrite powder, 1 wt% Poly Ethylene Imine (PEI) (Alfa Aesar-99%, 10 000 Molecular Weight) and 1 wt% Poly Vinyl Butyral-co-vinyl-alcohol-co-vinyl acetate (PVB) (Sigma Aldrich-50 000-80 000 Molecular Weight, 62-72 ºC Glass Transition Temperature) were prepared with variable amount of Phosphate Ester (PE) (Alfa Aesar-98%) in separate beakers. At first, the suspensions were homogenized with an ultrasonic probe for about half an hour. The

suspensions were balled milled with zirconia balls for 24 hours followed by agitation in an ultrasonic bath for 30 minutes. The pH and zeta potential of the suspensions were recorded using pH meter from Eutech Instruments and Zetasizer Nano ZS from Malvern, respectively.

Figure 3.2: Ultrasonic probe used in homogenizing suspension.

Figure 3.3: Horizontal ball mill used for homogeneous mixing in suspension.

Figure 3.4: Ultrasonic cleaning bath.

3.2.2 Percentage of Ferrite Powder, Binder & Dispersant

The amount of ferrite powder required for EPD was manipulated in separate tests, namely, 0.1 wt%, 0.3 wt% and 0.5 wt% in order to study the effect of solid loading in suspension. These suspensions were mixed in ethanol with proper amount of PE as charging agent, 1 wt% of PEI as dispersant and 1 wt% of PVB as binder. The suspensions were homogenized with an ultrasonic probe for about half an hour. The suspensions were balled milled with zirconia balls for 24 hours to insure homogeneous mixing. The suspension was then sonicated in an ultrasonic bath for 30 minutes. The pH and viscosity of the suspensions were measured using pH meter from Eutech Instruments and SV-10 Vibro Viscometer from A&D Company respectively. The zeta potential and the electrophoretic mobility of the suspensions were measured using Zetasizer Nano ZS from Malvern. The suspensions were left for a day to observe the sedimentation.

3.3 EPD Experiment

Based on all the previous results, using the optimal suspension with proper amount of ferrite powder, wt% of charging agents, binder and dispersant, EPD experiment was carried out using suitable electrodes and a proper connection to a stable DC voltage supplier.

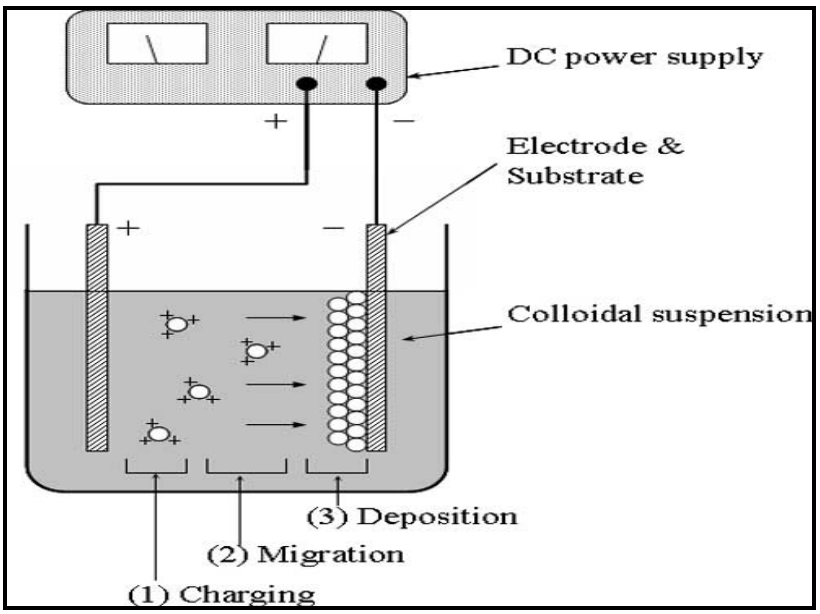

Figure 3.5: Schematic illustration of EPD experimental setup (Hashi *et al*, 2004).

Prior to manipulation of EPD parameters, a suitable suspension must be determined. A suspension with 80 ml (99.9 wt%) of ethanol, 63.2 mg (0.1 wt%) of ferrite powder, 0.632 mg (1 wt%) of PVB as binder, 0.591 µl (1 wt%) of PEI as dispersant and 2.582 µl (4 wt%) of phosphate ester as charging agent was prepared and EPD were performed.

3.3.1 Electrode Materials

Copper plates and stainless steel plates were prepared in pairs with a deposition area of 20 mm x 25 mm as an anode and deposition area of 10 mm x 25 mm as a cathode. It is important that the electrodes are polished and cleaned before being used in EPD process because the surface impurities might affect the adherence and strength of the deposit. After cleaning with dilute hydrochloric acid, electrodes were rinsed with distilled water and dried in a vacuum oven for 15 minutes.

The electrodes were placed vertically and parallel, the distance between the electrodes was fixed at 10 mm and submerged in the prepared suspension. A voltage source, DC power supply (Apparatus Corporation), was used for applying the electric field. The source was capable of performing either as a constant current or as a constant voltage source. A voltage of 200 V was applied for one hour. During deposition, a very small current of about 1 mA was observed. After EPD, the film was removed from the colloidal suspension and allowed to dry at room temperature for 24 hours. Deposit weights were obtained by weighing the electrode before and after deposition experiments. The adherence of the deposit and surface profile were observed visually and compared.

3.3.2 Voltage Variation

Similarly, the experiment to determine the most appropriate voltage to be used in further tests requires a fixed suspension system. Again, a suspension with 80 ml (99.9 wt%) of ethanol, 63.2 mg (0.1 wt%) of ferrite powder, 0.632 mg (1 wt%) of PVB as binder,

0.591 µl (1 wt%) of PEI as dispersant and 2.582 µl (4 wt%) of phosphate ester as charging agent was used. Stainless steel electrodes were used and electrode separation distance was standardized at 10 mm. Voltages of 100 V, 200 V and 300 V were manipulated in three separate tests. Deposition time was fixed as one hour. Deposit weights were obtained by weighing the electrode before and after deposition experiments. The adherence of the deposit and surface profile were observed and compared.

3.3.3 Electrode Separation Distance

Using the same suspension system with stainless steel electrodes, voltage applied was fixed at 200 V and deposition time of one hour. The electrode separation distances were varied at 10 mm and 20 mm. Again, deposit weights were obtained by weighing the electrode before and after deposition experiments. The adherence of the deposit and surface profile were observed and compared.

The deposition with the most suitable EPD parameters was sintered in a tube furnace in inert atmosphere for 2 hours at 1000 ºC. The ferrite films were examined under Gemini Field Emission Scanning Electron Microscope (FE-SEM) from Zeiss, Philips PW 3040 X-Ray Diffractometer (XRD) and Ambios Q-Scope Scanning Probe Microscope.

3.4 Materials Characterization

A variety of characterization techniques were employed in this study to analyze the ferrite layers deposited by EPD as well as to evaluate powder and suspension characteristics. The materials characterization includes the analyses from TGA, TEM, AGM, Zetasizer, Viscometer, FE-SEM, EDX, XRD, AFM and MFM.

Mettler SDTA851e Thermogravimetry Analysis (TGA) is an analytical technique used to determine thermal stability of a material and its fraction volatile component by monitoring the weight change that occurs as the specimen is heated. As materials are heated, they can lose weight from a simple process such as drying, or form chemical reactions that liberate gases. Some materials can gain weight by reacting with the atmosphere in the testing environment. Since the weight loss and gain are disruptive processes to the sample material, knowledge of the magnitude and temperature range of those reactions are necessary in order to design adequate thermal ramps and holds during those critical reaction periods (Internet Reference, 10/10/2009). Nickel zinc ferrite powder and magnesium copper zinc ferrite powder produced by water-in-oil microemulsion method were sent for TGA analysis to determine the calcination temperature. A graph of weight loss as a function of temperature is plotted by the computer so called thermogravimetry curve. The thermal stability is studied from the graph.

LEO-Libra 120 Transmission Electron Microscope (TEM) was used to measure the particle size of the ferrite powder. It is suitable equipment because it has a broad

measuring range of 0.02 μm to 2000 μm. Besides, samples in the form of emulsions, suspensions and dry powder can be examined with this TEM. It is crucial to determine the particle size of the particulate precursor in the suspension as it affects the deposition strength and thickness as well. Larger range of particle sizes can also be detected over the range of results posted from the TEM analyses, of which it poses possibilities of agglomeration among the particles (Internet Reference, 11/10/2009a).

The magnetic properties of the ferrite powders are investigated using alternating gradient magnetometer (AGM). AGM is a very sensitive system for measuring magnetic hysteresis parameters at room temperature. The magnetic sample is mounted on the end of a cantilevered rod that incorporates a piezoelectric element. The alternating field exerts an alternating force on the sample, resulting in a deflection of the sample within the field. The resulting deflection of the cantilevered rod is measured by the voltage output of the piezoelectric elements. Output signals are detected by build-in software and processed through a computer. The gradient field strength alternating from a maximum of 10 kOe to a minimum of -10 kOe is exerted on the sample. Around 0.5 mg powders are weighed and placed onto a double-sided tape. The specimen is then attached to the transducer probe and the measurement is performed.

The Zetasizer (Malvern Instruments) equipment is used to measure the particle size and zeta potential of the suspension to optimize stability, shelf life and speed up formulation development (Internet Reference, 11/10/2009c). The surface properties that closely relate to particle size and surface charge determine the dispersion characteristics

in the suspension. If all the particles in suspension have either a large negative or positive zeta potential then they will tend to repel each other and there is no tendency to flocculate. However, if the particles have low zeta potential values then there is no force to prevent the particles coming together and flocculating (Besra *et al*, 2007).

Viscosity of suspension was measured using Vibro Viscometer (A&D Company Limited). Sine-wave Vibro Viscometer SV-10 measures viscosity by detecting the driving electric current necessary to resonate the two sensor plates at constant frequency of 30 Hz and amplitude of less than 1 mm (Internet Reference, 11/01/2011). Measurement involves lowering the sensors into the sample, pressing the start button on the control unit, and then waiting just 15 seconds for the result to be displayed.

Zeiss' Gemini Field Emission Scanning Electron Microscope (FE-SEM) was used to characterize the microstructures of the deposit on the electrode substrate. FE-SEM is capable of producing ultra high resolution images of a sample surface at both low and high acceleration voltages. A wide range of magnification imaging is suitable to identify the porosity and presence of other impurity structures in the deposit. FE-SEM's variable pressure (VP) capability enables examination of non-conducting specimens without time consuming preparation. The new technology in the Gemini electron optical column gives high resolution imaging SEM with optimised analytical capabilities for Energy Dispersive X-Ray Spectroscopy (EDX) nanoanalysis. EDX is an analytical technique used for the elemental analysis or chemical characterization of a sample. As a type of spectroscopy, it relies on the investigation of a sample through interactions between

electromagnetic radiation and matter, analyzing X-rays emitted by the matter in response to being hit with charged particles. Its characterization capabilities are due in large part to the fundamental principle that each element has a unique atomic structure allowing X-rays that are characteristic of an element's atomic structure to be identified uniquely from each other (Internet Reference, 11/10/2009b). FE-SEM was used in conjunction with energy dispersive X-ray spectroscopy to determine the composition of the deposited ferrite layer.

Philips PW 3040 X-Ray Diffraction (XRD) is a versatile non-destructive technique that reveals detailed information about the chemical composition and crystallographic structure of the natural and manufactured materials. It uses the X-ray or neutron diffraction on specimen. The deposited ferrite layers from EPD process were sent for XRD analysis to determine the phase composition

Ambios Q-Scope Scanning Probe Microscope (SPM) is a technique where a fine probe mounted on a piezoelectric x, y and z scanner (called the cantilever), makes a scan over a surface which can reveal images down to atomic level. Utilizing a scanning probe microscope in both atomic and magnetic imaging mode, known as atomic force microscopy (AFM) and magnetic force microscopy (MFM) respectively enable to differentiate between magnetic and non magnetic phases in materials. MFM imaging mode is based on non-contact Atomic Force Microscopy (AFM), with the tip modulated at or near its resonant frequency by means of a piezoelectric element and the cantilever coated with a magnetic material. When resonated over the sample surface, the

tip–sample interaction includes both surface and magnetic forces. MFM is the experimental technique to study the fringing field above magnetic materials. The principal idea of this method relies on the magnetostatic interaction between the magnetic sample and the magnetic sensor attached to a cantilever and placed tens or hundreds of nanometers over the sample. The magnetic characteristics in ferrite regions can be distinguished by comparing the AFM and MFM images.

CHAPTER 4

RESULTS & DISCUSSION

4.1 Nano Powder Analyses

Nickel zinc ferrite and magnesium copper zinc ferrite powders produced by water-in-oil microemulsion consist of two concurrent reactions relying on hydroxide ion concentration. Formation of goethite (α-FeOOH) occurred for the first reaction. The second reaction is associated with the oxidation of hydroxide and incorporation of Fe^{3+} into the ferrite compound (Thakur *et al*, 2009). The precipitation of nickel zinc ferrite by water-in-oil microemulsion occurred according to the following reactions:

$2Fe^{2+} + 4OH^- + 0.5O_2 \rightarrow 2FeOOH + H_2O$

$0.5Ni^{2+} + 0.5Zn^{2+} + 2Fe^{2+} + 6OH^- + 0.5O_2 \rightarrow Ni_{0.5}Zn_{0.5}Fe_2O_4 + 3H_2O$

Whereas simplified chemical reactions for producing magnesium copper zinc ferrite can be written as

$2Fe^{2+} + 4OH^- + 0.5O_2 \rightarrow 2FeOOH + H_2O$

$0.09Mg^{2+} + 0.34Cu^{2+} + 0.57Zn^{2+} + 2Fe^{2+} + 6OH^- + 0.5O_2 \rightarrow Mg_{0.09}Cu_{0.34}Zn_{0.57}Fe_2O_4 + 3H_2O$

The ferrite powders were characterized using TGA, TEM and AGM. The synthesized ferrites were then used in the subsequent EPD processes.

4.1.1 Thermogravimetry Analysis (TGA)

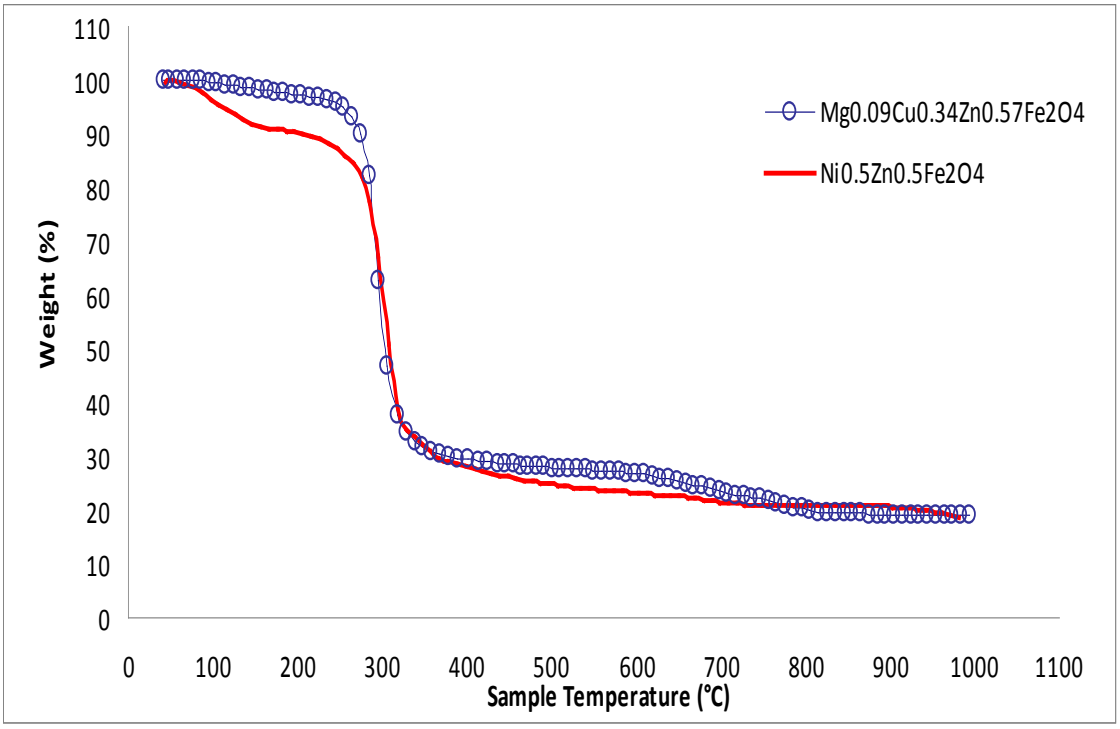

Figure 4.1: Thermograms of nickel zinc ferrite and magnesium copper zinc ferrite.

TGA test was performed to determine the calcination temperature of the ferrite samples. Figure 4.1 shows the thermograms of $Ni_{0.5}Zn_{0.5}Fe_2O_4$ (nickel zinc ferrite) and $Mg_{0.09}Cu_{0.34}Zn_{0.57}Fe_2O_4$ (magnesium copper zinc ferrite), where both samples have similar weight loss characteristics. The weight loss for both samples began from room temperature to 250 °C, which is attributed to the dehydration of hydroxide complexes. The second degradation process occurred at around 600 °C to 800 °C and 825 °C to 1000 °C for $Mg_{0.09}Cu_{0.34}Zn_{0.57}Fe_2O_4$ and $Ni_{0.5}Zn_{0.5}Fe_2O_4$ respectively. It indicates the ferritization process – a process where formation of ferrite takes place. As a result, $Mg_{0.09}Cu_{0.34}Zn_{0.57}Fe_2O_4$ and $Ni_{0.5}Zn_{0.5}Fe_2O_4$ are scheduled for calcination at 700 °C and 900 °C respectively for one hour with a heating rate of 4 °C/min to ensure the complete dehydration and decomposition of the hydroxide complexes to form ferrite. The heating

rate and duration of calcination were chosen to ensure homogeneous heating within the samples and also to prevent excessive self-heating which will lead to lack of chemical homogeneity and agglomeration.

4.1.2 Transmission Electron Microscope (TEM)

Figure 4.2 – 4.5 show TEM images and size distribution histogram of the nickel zinc ferrite and magnesium copper zinc ferrite nanoparticles.

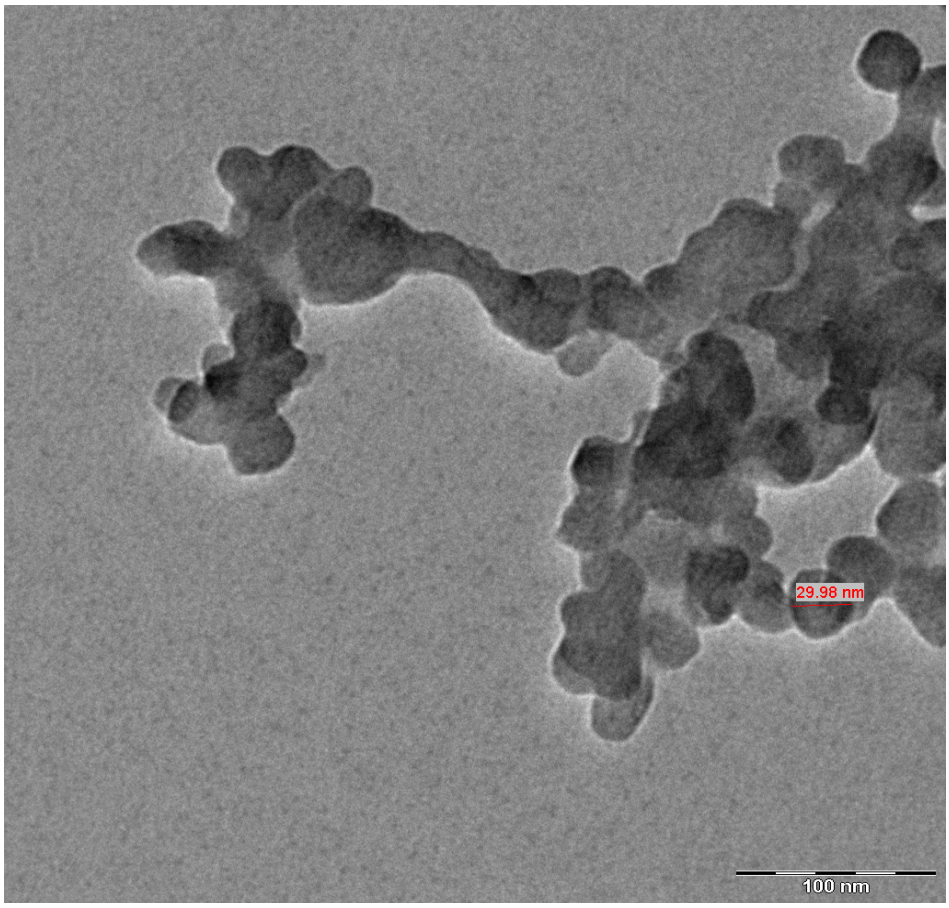

Figure 4.2: Transmission electron micrograph showing the microstructure of nickel zinc ferrite nanoparticles.

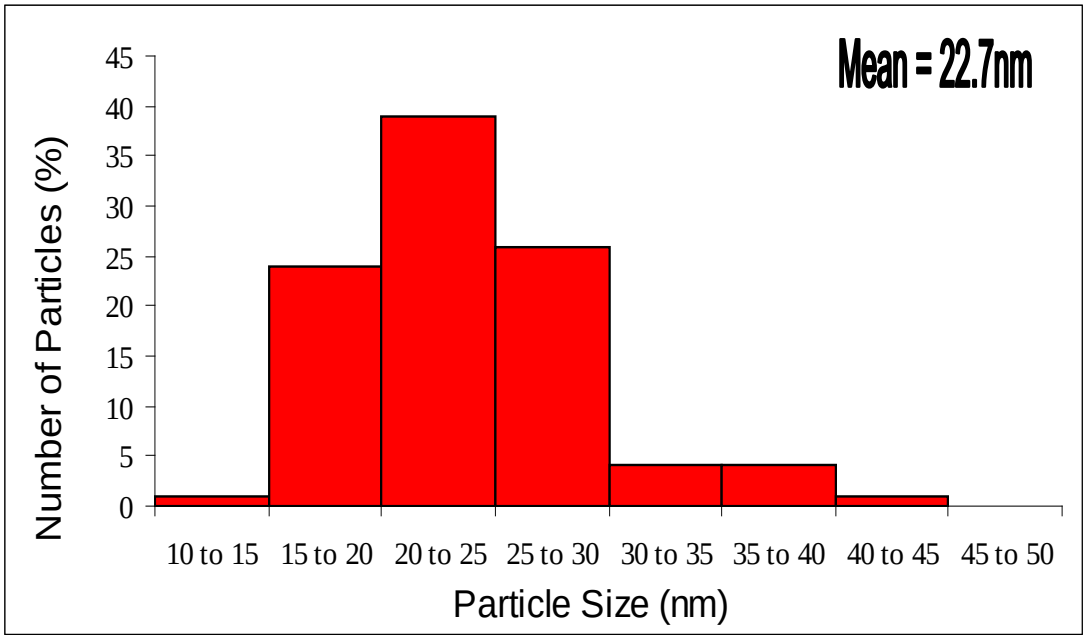

Figure 4.3: Histogram of the particle size distribution obtained from nickel zinc ferrite nanoparticles.

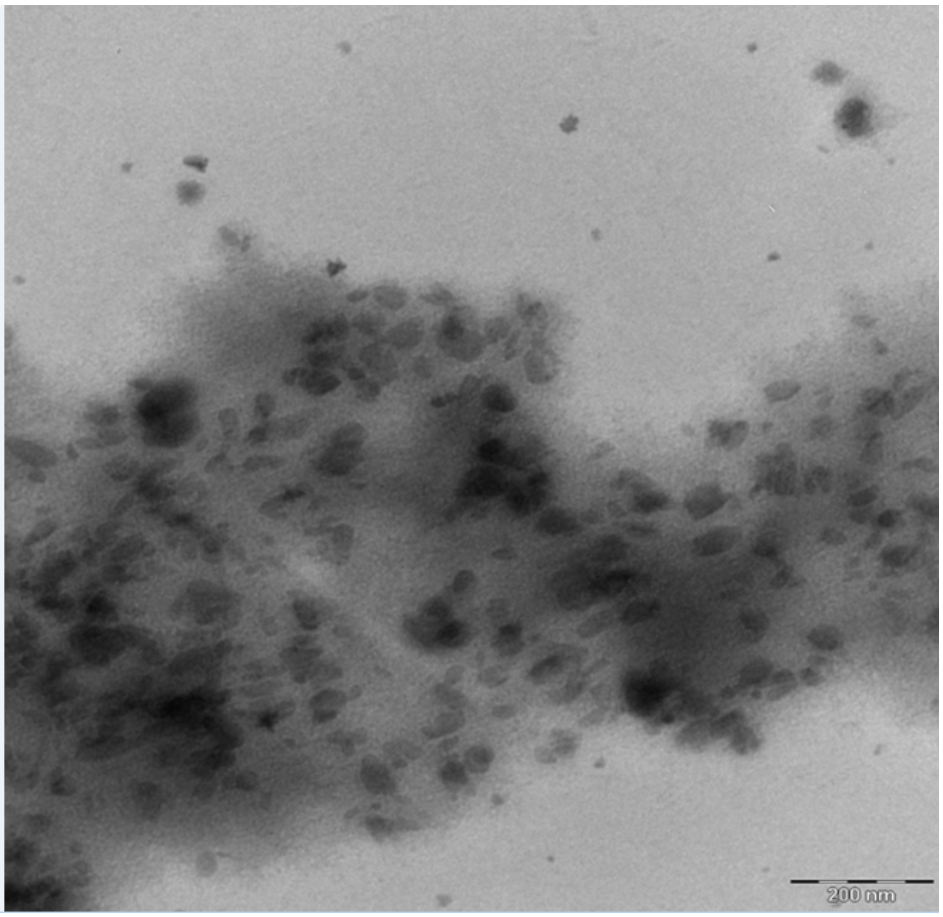

Figure 4.4: Transmission electron micrograph showing the microstructure of magnesium copper zinc ferrite nanoparticles.

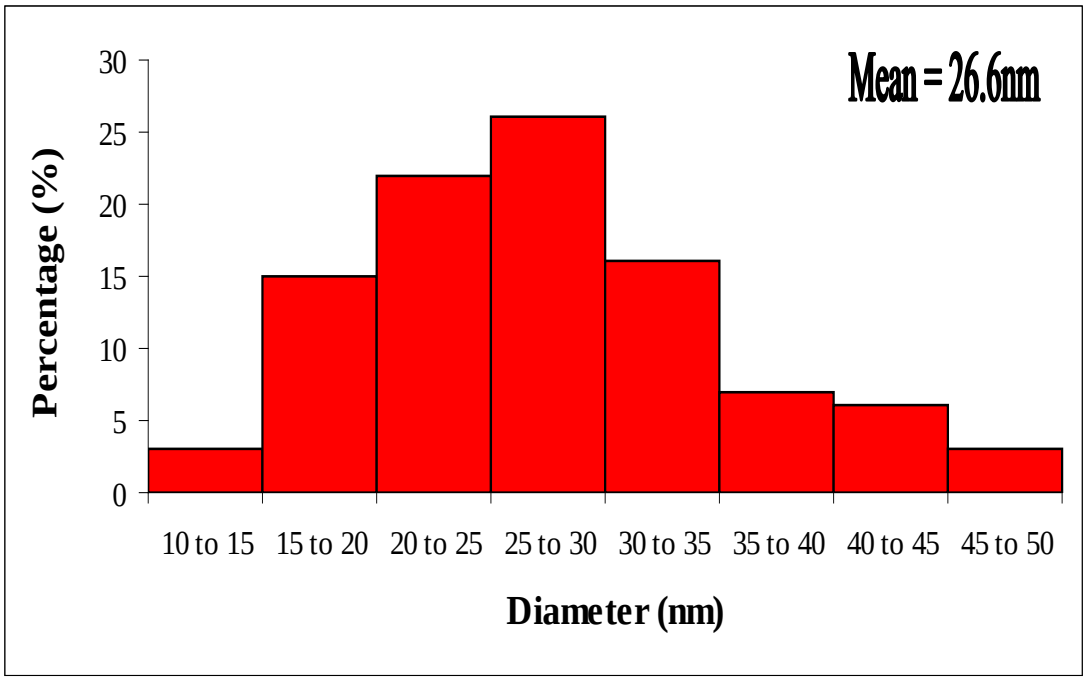

Figure 4.5: Histogram of the particle size distribution obtained from magnesium copper zinc ferrite nanoparticles.

TEM studies in atomic resolution and electron diffraction have revealed that the synthetic $Ni_{0.5}Zn_{0.5}Fe_2O_4$ nanoparticles are roughly spherical in shape and $Mg_{0.09}Cu_{0.34}Zn_{0.57}Fe_2O_4$ nanoparticles have irregular shape. $Ni_{0.5}Zn_{0.5}Fe_2O_4$ nanoparticles have a more uniform size distribution compared to $Mg_{0.09}Cu_{0.34}Zn_{0.57}Fe_2O_4$ nanoparticles. The average size of $Ni_{0.5}Zn_{0.5}Fe_2O_4$ and $Mg_{0.09}Cu_{0.34}Zn_{0.57}Fe_2O_4$ nanoparticles is 22.7 nm and 26.6 nm respectively, and this was calculated by measuring the diameters of 100 particles. The size of the product particles is affected by the concentration of the reactants in the aqueous solution of reverse micelles (Palmqvist, 2003). The particle size of magnesium copper zinc ferrite is slightly higher than that of nickel zinc ferrite due to the higher reactant concentration in Mg-Cu-Zn ferrite. The size of spherical nanoparticles is controlled by employing low water contents (W = [water]/[surfactant]) (Caragheorgheopol *et al*, 2004). In other

words, lower water contents were used in the synthesis process of nickel zinc ferrite particle and consequently resulted in smaller particle size produced.

4.1.3 Alternating Gradient Magnetometer (AGM)

For magnetic measurements, nickel zinc ferrite and magnesium copper zinc ferrite powders were calcined at 900 °C and 700 °C respectively for one hour in tube furnace in inert atmosphere for complete ferritization process. The calcined ferrites powders were then characterized using alternating gradient magnetometer.

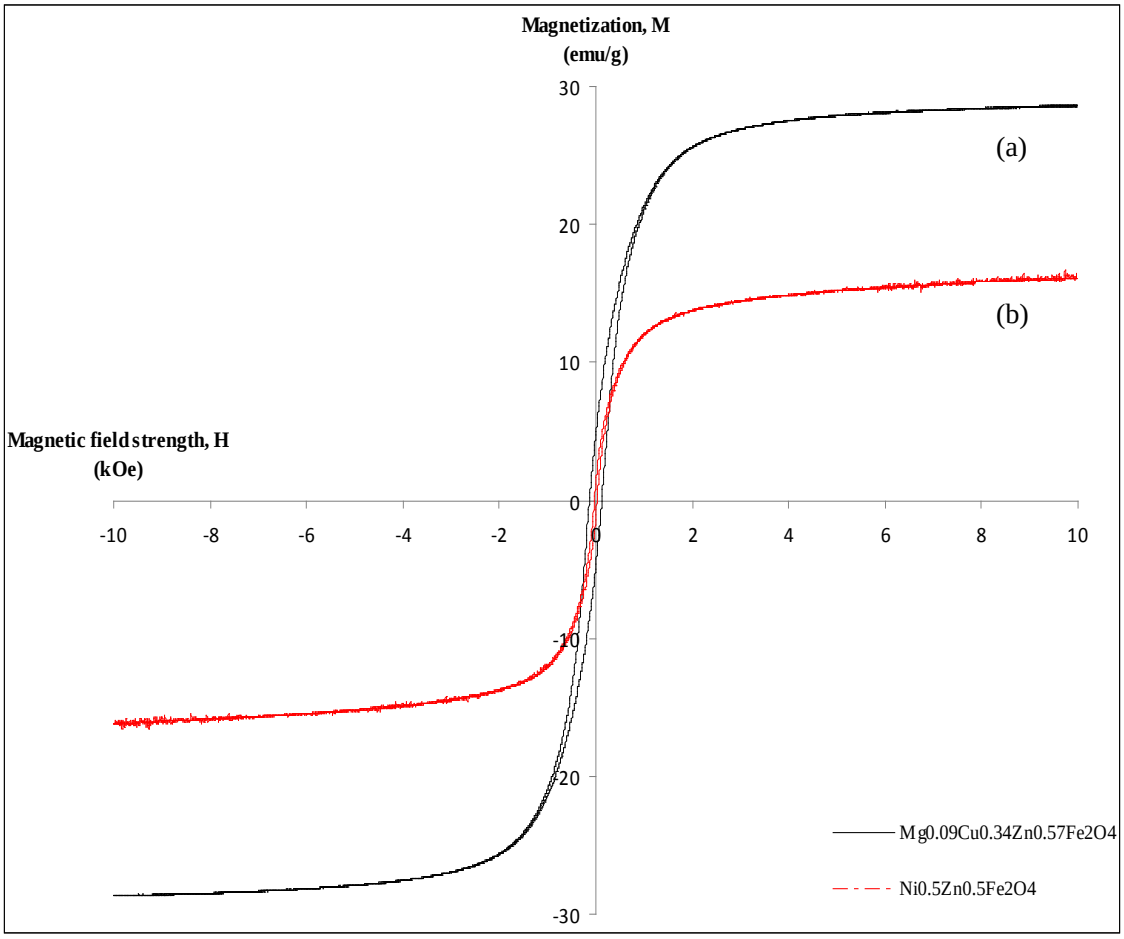

Figure 4.6: Magnetization curves of calcined (a) magnesium copper zinc ferrite and (b) nickel zinc ferrite nanoparticles.

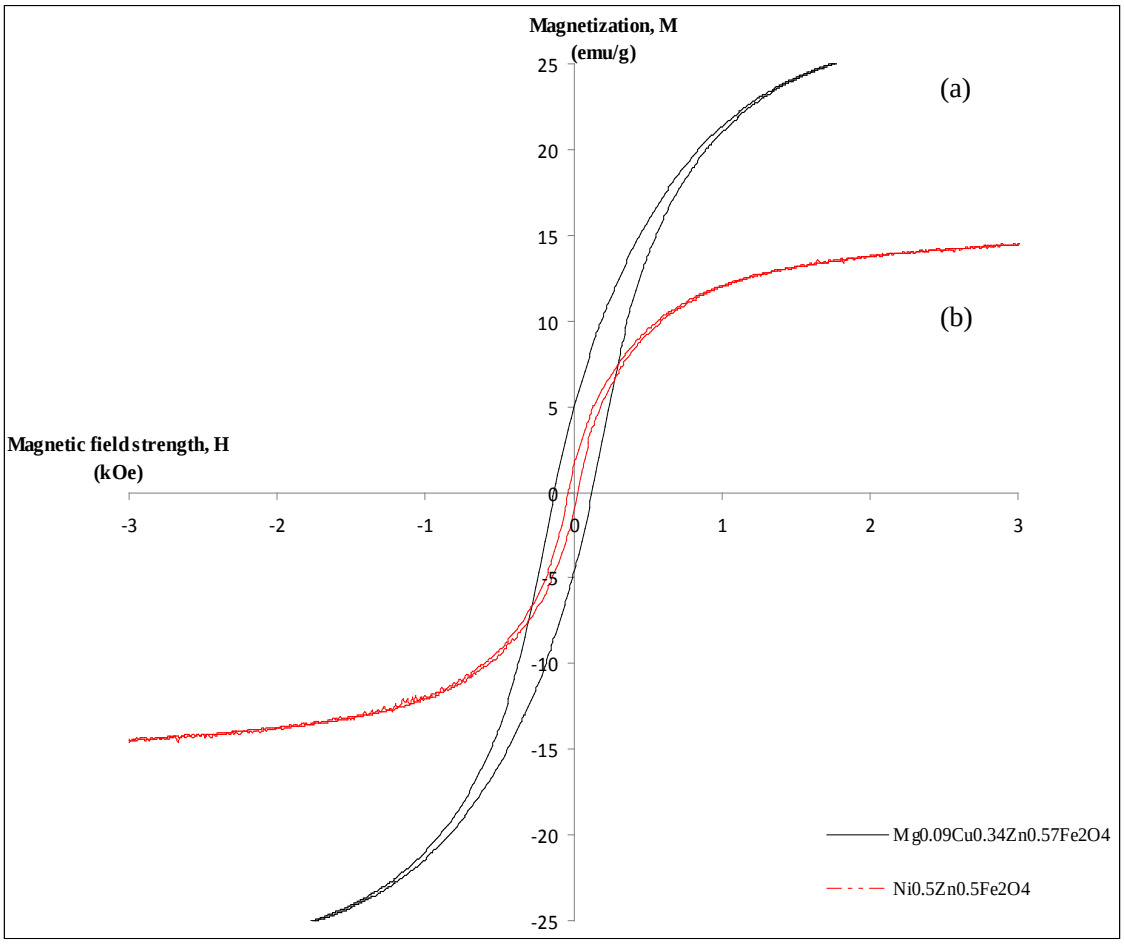

Figure 4.7: Magnetic hysteresis loop of calcined (a) magnesium copper zinc ferrite and (b) nickel zinc ferrite nanoparticles.

Table 4.1: Magnetic properties for calcined magnesium copper zinc ferrite and nickel zinc ferrite nanoparticles

Samples	**$Mg_{0.09}Cu_{0.34}Zn_{0.57}Fe_2O_4$**	**$Ni_{0.5}Zn_{0.5}Fe_2O_4$**
Coercivity, Hc (Oe)	126.0	25.50
Saturation Magnetization, Ms (emu/g)	28.66	16.10
Remanence of Magnetization, Mr (emu/g)	5.030	1.674
Mr/Ms	0.176	0.100

Figure 4.6 presents the magnetic hysteresis curves of the calcined (a) $Mg_{0.09}Cu_{0.34}Zn_{0.57}Fe_2O_4$ and (b) $Ni_{0.5}Zn_{0.5}Fe_2O_4$ nanoparticles. Figure 4.7 shows the larger version of magnetic hysteresis loop of the ferrites nanoparticles. The M-H (magnetization versus magnetic field strength) curve of MgCuZn ferrite shows a slightly larger hysteresis loop compared to that of NiZn ferrite. The coercivity values for MgCuZn ferrite and NiZn ferrite are 126 Oe and 25.5 Oe respectively. This shows a soft ferromagnetic behaviour. For nanocomposite materials, the soft magnetic properties originate from the intergrain interaction because of the exchange coupling of the neighbouring magnetic nanoparticles. The intergrain interaction tends to average the anisotropy of each individual particle, resulting in much reduced anisotropy and, subsequently, higher permeability (Kurinec et al, 2006). A lower value of coercivity for nickel zinc ferrite enhances the electromagnetic properties. This is because the low value of coercivity corresponds to the easy movement of domain walls as the magnetic field changes magnitude and direction. The reduction in coercivity value for nickel zinc ferrite will cause an increase in permeability and consequently a decrease in hyteresis loss. Generally low hysteresis loss is a desirable characteristic of soft magnetic materials (Jiles, 2003).

The saturation magnetization values for $Mg_{0.09}Cu_{0.34}Zn_{0.57}Fe_2O_4$ and $Ni_{0.5}Zn_{0.5}Fe_2O_4$ are 28.66 emu/g and 16.10 emu/g respectively. The higher magnetization value of magnesium copper zinc ferrite is attributed to the high phase purity and well-defined crystallinity of its phase. In the late sixties, Berkowitz and co-workers has proved that magnetization value at room temperature decreases sharply

with decreasing crystalline size (Berkowitz, 1968). The smaller size range of NiZn ferrite causes the magnetization value to be lower. It is therefore verified that MgCuZn ferrite produced from water-in-oil microemulsion shows better magnetic property than NiZn ferrite. Magnetic property of the synthesized ferrites is greatly influenced by the structure of its phase formed.

4.2 Suspension Analysis

Prior to performing EPD, it is important to quantitatively characterize the colloidal dispersion utilized in the process. Suspensions of ferrite were prepared by dispersing ferrite powder in ethanol and mixing of additives such as PE, PEI and PVB. Additives will influence the stability of the suspensions. Phosphate ester (PE) is an effective charging agent which provides stabilization of ferrite particles in suspension. PVB acts as binder to improve the binding properties on the electrode during EPD. PEI is functioning as a dispersant. The deposition time for the EPD experiments performed in this study was one hour or less. Thus, it was critical that the stability of the dispersion be observed within this time frame.

The following experiments were conducted to characterize the suspension and deposition properties using the ethanol suspensions prepared with PE as charging agent, 1 wt% PVB as binder and 1 wt% PEI as dispersant. In the following segments, the amount of charging agent was manipulated as a function of zeta potential, pH and conductivity of the suspension. The effect of solid concentration was studied by varying the weight percentage of ferrite powder in the suspension with 0.1 wt%, 0.3 wt% and

0.5 wt%.

4.2.1 Zeta Potential Analysis

The experiments on zeta potential analysis were based on suspensions with 1 wt% (99 wt% ethanol) of ferrite powders. Based on the results obtained from the Zetasizer, the zeta potential, conductivity and pH were compared as a function of weight percentage of Phosphate Ester. Below are the results and graphical representation with different volume of PE used for each suspension system.

Table 4.2: The average zeta potential values based of different amount of PE used for each suspension system

wt% PE	Volume of PE used (μl)	Average Zeta Potential (mV)
1	0.6456	12.6
2	1.291	12.0
3	1.937	11.2
4	2.582	12.8
5	3.228	11.7
6	3.873	11.4
7	4.519	10.3
8	5.164	12.0
9	5.810	10.7
10	6.456	11.1

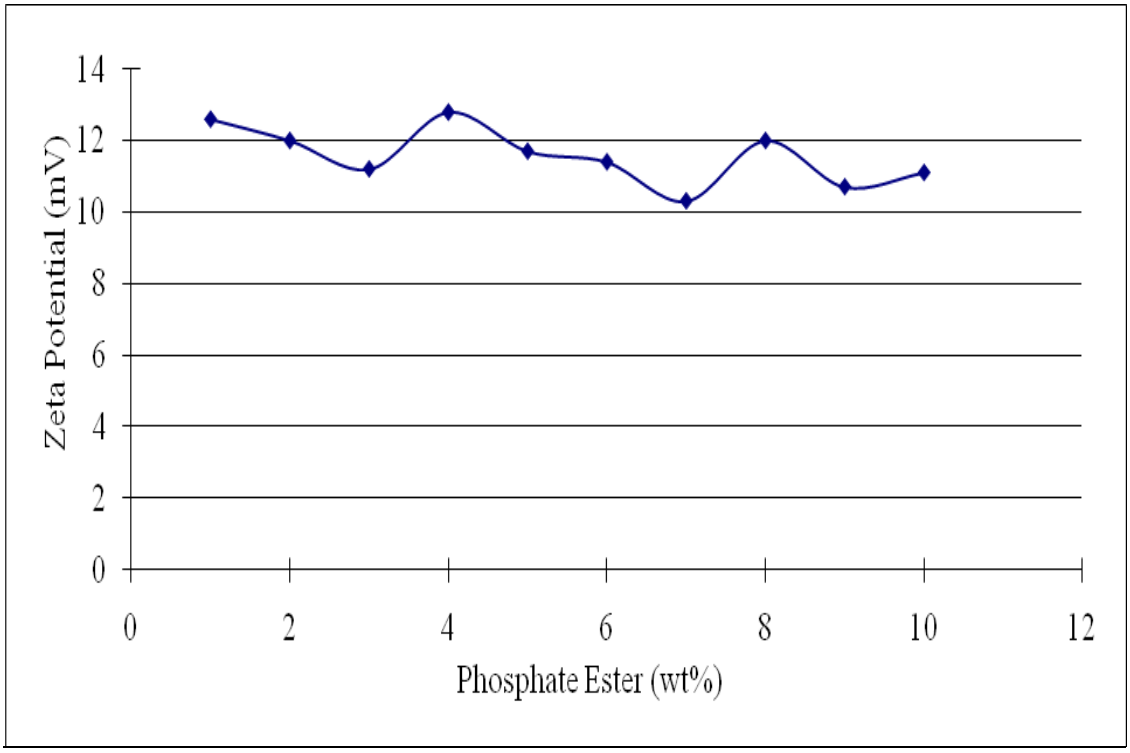

Figure 4.8: Graph of average zeta potential versus weight percentage of Phosphate Ester for suspension with 1 weight percentage of ferrite powder.

As shown in Figure 4.8, the zeta potential values decrease from 1 wt% of PE to 3 wt% of PE but increase to the first maximum zeta potential value at about 4 wt% of PE (~12.8 mV). The first minimum zeta potential value was recorded to be at approximately 7 wt% PE (~10.3 mV) and the curve rose again. This phenomenon can be explained based on the amount of PE used. PE or butyl acid phosphate used in this study is a mixture of mono- and di-esters. They dissociate in ethanol or any other organic solvent and produce charged ions. The protons (hydronium ions, H+) are released from the PE and adsorb onto the ferrite powder and positively charge the powder surface. Hence this explains the increase in zeta potential value.

As the amount of PE continuously increased, total adsorbed protons became gradually saturated and the dissociation of PE reached the equilibrium state. Hence, PE stopped dissociating and the excess PE molecules were present in the neutral state in the suspension. The zeta potential value dropped to 7.08 mV when the concentration of PE reached 60 wt%. As a result, excessive addition of PE, as expected, caused a subsequent decrease in the zeta potential.

4.2.2 pH Variation & Conductivity Measurements

The pH variation and conductivity measurements with different amount of PE were recorded and analyzed.

Table 4.3: The pH and conductivity values based on different amount of PE used for each suspension system

wt% PE	Volume of PE used (μl)	pH	Conductivity (mS/cm)
1	0.6456	10.84	0.0379
2	1.291	10.81	0.0406
3	1.937	10.84	0.0425
4	2.582	10.80	0.042
5	3.228	10.80	0.0421
6	3.873	10.70	0.0418
7	4.519	10.65	0.0427
8	5.164	10.71	0.0433
9	5.810	10.68	0.0462
10	6.456	10.64	0.0452

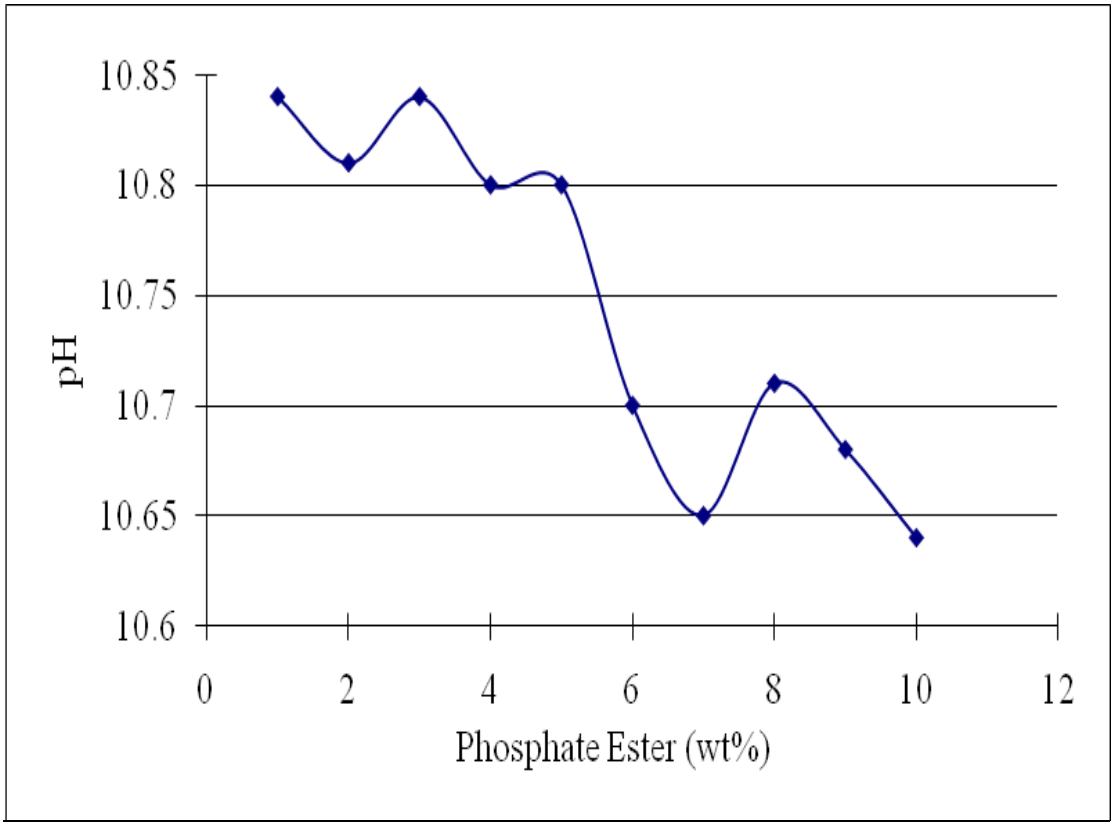

Figure 4.9: Graph of pH versus weight percentage of Phosphate Ester for suspension with 1 weight percentage of ferrite powder.

An overview in Figure 4.9, pH decreases from 11 to 10 for 1 wt% PE to 10 wt% PE. pH values do not have significant impact on increasing amount of charging agent. When the concentration of PE reached 60 wt%, a pH value of 11 is obtained. Excessive addition of PE does not affect much on the pH value because the amount of ferrite powder is fixed with 1 wt%. pH value would not drop when the amount of ferrite particles presented in the suspension are all being mobilized by the excessive hydronium ions produced from the charging agent PE.

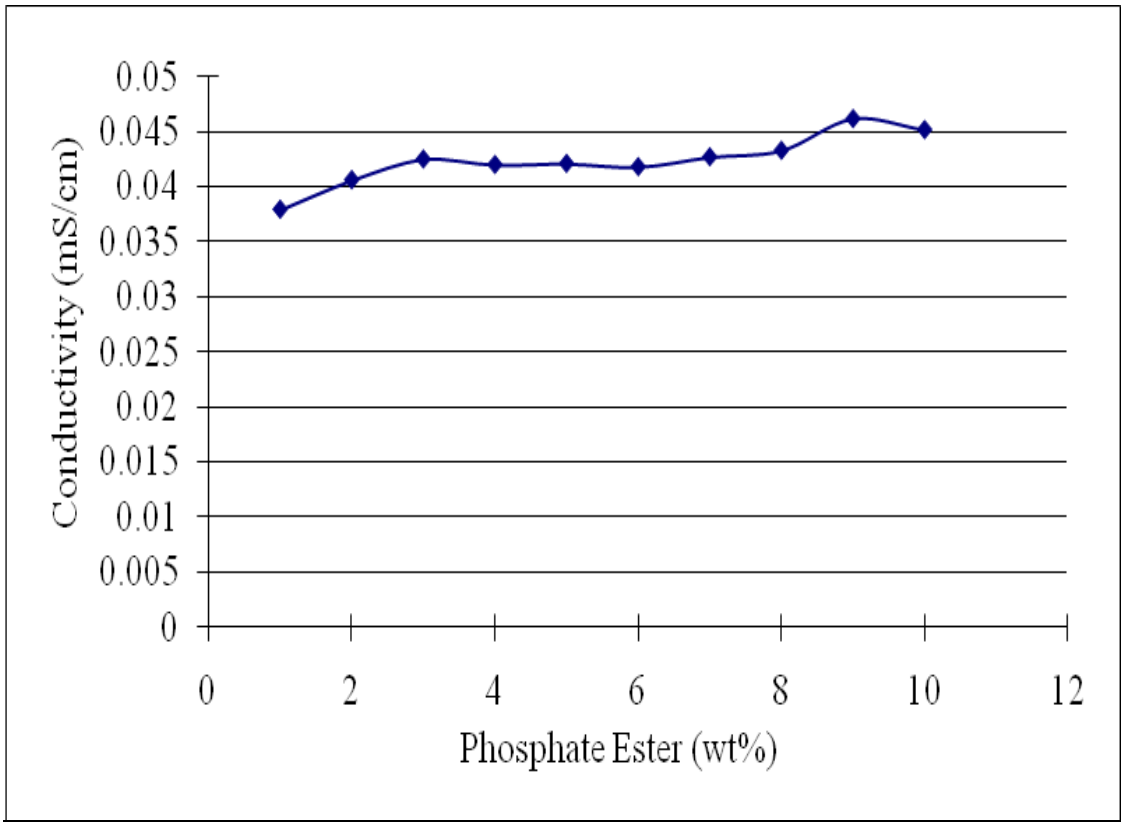

Figure 4.10: Graph of conductivity versus weight percentage of Phosphate Ester for suspension with 1 weight percentage of ferrite powder.

The conductivity curve is shown in Figure 4.10. There is a large increase from 1 wt% to 3 wt% of PE. This phenomenon can be explained in a similar manner as the previous one, based on the dissociation rate of PE. In the case of smaller amounts of PE, a high initial dissociation rate of PE greatly promotes an increase in conductivity. As the dissociation of PE reached an equilibrium state at higher PE content, the amount of adsorbed protons became saturated and the conductivity remained constant. Hence, a gentle slope at 9 wt% of PE in the end-span of the curve was observed. The conductivity value decreased to 0.0285 mS/cm with 60 wt% PE. This can be explained by the dissociation of PE reaching an equilibrium state; the conductivity value would start to drop with an excessive PE content. It can be concluded that as the amount of PE

increased (but not in the case of excessive PE content), more H+ are available in the suspension. Hence, the pH dropped and the electrical conductivity increased. However, the conductivity values for the colloidal suspension with different weight percentage of PE are very low. EPD suspensions that are relatively low in conductivity are ideal because they are incapable of changing the surface charges of the engrossed colloidal particles.

4.2.3 Effect of solid loading in suspension

The zeta potential value is highest for suspensions with 4 wt% PE. Hence, the experiments on the effects of solid loading were based on suspensions with 4 wt% PE, 1 wt% PVB, 1 wt% PEI. The weight percentage of ferrite powder was manipulated in the ethanol based suspensions with 0.1 wt%, 0.3 wt% and 0.5 wt%.

Table 4.4: Parameters variation for different weight percentage (wt%) of ferrite in suspension

	$Ni_{0.5}Zn_{0.5}Fe_2O_4$		
Solid Concentration (wt%)	**0.1**	**0.3**	**0.5**
Zeta Potential (mV)	34.4	33.2	15.3
Mobility (cm^2/Vs)	0.71	0.69	0.32
Viscosity (mPa.s)	1.15	1.17	1.24
Conductivity (mS/cm)	0.007	0.02	0.03
pH	10	9.8	9.7
Particle Size (nm)	584	607	774

*__Suspension composition__: 4 wt% PE, 1 wt% PVB, 1 wt% PEI

High absolute zeta potential value indicates a high degree of particle dispersion in the suspension. Ferrite particles developed the largest positive surface potential of about 34.4 mV at pH 10.01 with 0.1 wt% of solid loading. The positive value of zeta potential indicated that the prepared suspension is positively charged and that the ferrite nanoparticles will be deposited on the cathode during EPD. Results from zeta pontetial measurements indicate that the ferrite particles with 0.1 wt% of solid loading in the EPD medium are well-stabilized due to high repulsive forces. As shown in Table 4.4, the electrophoretic mobility of 0.1 wt% of solid loading in the stabilized ethanol suspension is the highest (~0.71 cm^2/Vs). Precisely, suspension of lower ferrite powder concentration has higher levels of control on the thickness and uniformity of the deposited films.

The viscosity of the suspension increased with the weight percentage of solid loading. The increased solid loading increases the number of particles in the suspension. As a result, the repulsive force between particles increasing as the solid concentration of ferrite powders increases. Stable suspensions with low viscosity value and higher zeta potential are considered to be very suitable for EPD process.

The conductivity value increases apparently with the weight percentage of ferrite powder dispersed in the suspension. Higher conductivities reduce the effectiveness of the electric field exerted on the particles in the suspension. Therefore, the mobility of the particles is reduced and the deposition rate is lower. The desired properties in the stable suspension are low viscosity, low conductivity and high dielectric constant (value

of zeta potential).

The measured pH of the suspensions decreased from pH 10 with 0.1 wt% ferrite powders to pH 9.7 with 0.5 wt% ferrite powder. Consequently, the equilibrium reaction between the absorbed and free protons on the surface of each ferrite particle depends on the particle concentration. Suspended particles at lower concentration values were characterized by a relatively high and positive surface charge.

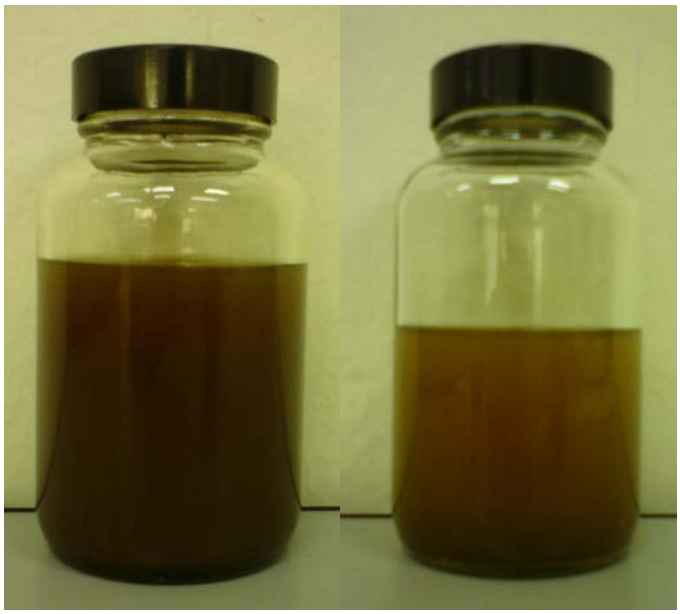

Figure 4.11: Suspension with 0.1 wt% ferrite (left) and suspension with 0.5 wt% ferrite (right).

As shown in Figure 4.11, the sedimentation rate for suspension with 0.5 wt% ferrite powder is much faster than the suspension with 0.1 wt% ferrite powder. High solid loading induces strong magnetic interactions. These magnetic interactions cannot be permanently screened with the electrostatic repulsive interactions, resulting in the short

term stability of the suspension and finally to the agglomeration and sedimentation of the particles. From Table 4.4, it can be observed that particle size for suspension with 0.1 wt% ferrite powder is smaller compared to the suspension with 0.5 wt% ferrite powder. This is because colloidal particles with smaller size range tend to remain in suspension for long periods due to Brownian motion. Continuous hydrodynamic agitation is required for particles larger than 1 μm to remain in suspension. It is because larger particles tend to settle due to gravity. Hence, it is difficult to get uniform deposition from a sedimenting suspension of large particles.

4.3 Determination of Standard EPD Parameters

Prior to the manipulation of basic parameters, the most stable ferrite suspension was used to determine the suitability for deposition of ferrite particles via EPD. The suspension is mixed in ethanol with 0.1 wt% ferrite powders, 4 wt% of PE as charging agent, 1 wt% of PVB as binder and 1 wt% of PEI as dispersant.

4.3.1 Effect of Electrode Materials

EPD was performed with 200 V of supply voltage and 10 mm electrode separation distance for one hour deposition. Two different types of electrodes were examined and observed to determine the most suitable to be used for depositing ferrite layers via EPD. Figure 4.12 shows the observation from two separate tests.

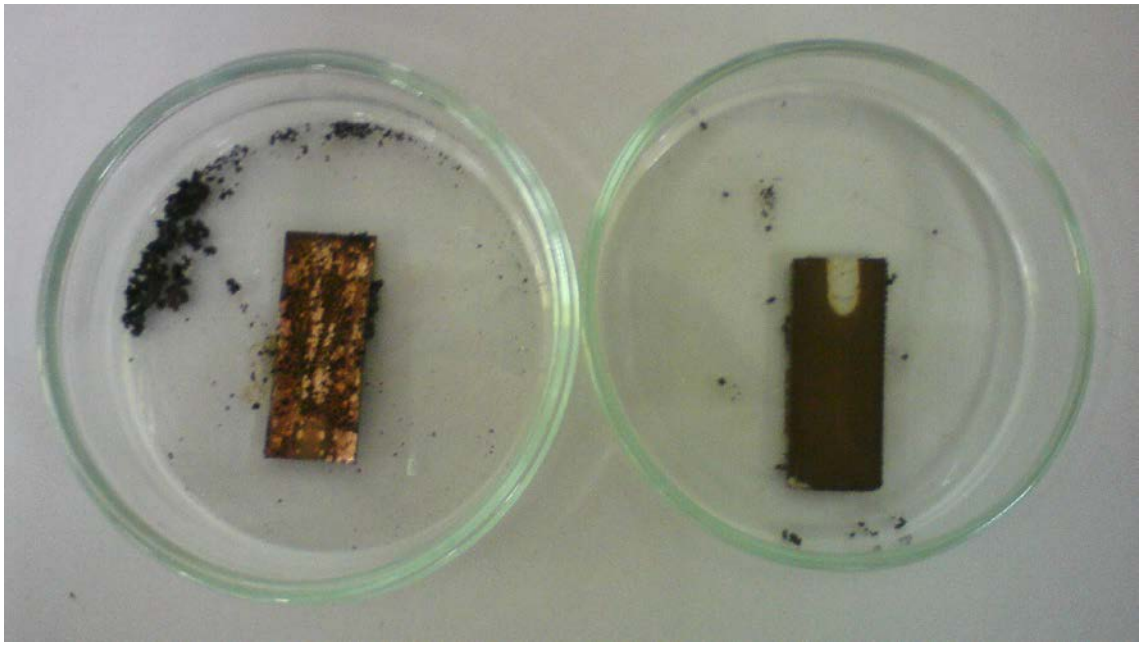

Figure 4.12: Ferrite layer deposition on copper plate (left) and stainless steel electrode (right).

Table 4.5: Observation of ferrite layers deposited via EPD for two different electrodes

Electrodes	Weight (mg)	Observation
Copper	2.8	Uneven deposition, weak adherence
Stainless Steel	8.1	Thin deposition with strong adherence to the substrate

As shown in Figure 4.12, it can be seen that the copper plate produced weakly adhered deposit and also, the deposition is less and spreaded unevenly. Stainless steel plate is capable in producing a more homogeneous deposit and thus more effective in EPD process. Weight of ferrite layer deposited using stainless steel electrodes is four times higher than the weight of ferrite layer deposited using copper plates. Copper plates which have higher thermal conductivity value (~385 W/m-K) hinder the particle

movement to be further deposit on the electrode during EPD. One limitation to use stainless steel plates as electrodes for EPD is Fe-matrix is present in stainless steel plates. Material characterizations like EDX would be not suitable simply because the Fe-matrix will predominate the test results. On the other hand, copper electrodes which have a melting point of 1085 °C could post a threat during sintering operations. As sintering is done at a maximum temperature of 1000 °C which is close to the melting point of copper electrodes. In addition, copper electrodes require a very inert sintering environment to prevent oxidation and other chemical reaction to take place. Stainless steel electrodes require less inert environment and economical nitrogen or argon gases were flushed in the tube furnace for sintering purpose.

4.3.2 Effects of Voltage Variation

Applied potential field were manipulated in three separate EPD processes. EPD was performed using stainless steel electrodes with 10 mm electrode separation distance for one hour deposition. The results and observation were as follows:

(a) (b) (c)

Figure 4.13: Deposited ferrite layers prepared at various supply voltage: (a) 100 V; (b) 200 V; (c) 300V.

Table 4.6: Observation of ferrite layers deposited via EPD for three different voltages

Voltages (V)	**Weight (mg)**	**Observation**
100	4.2	Slow process and very thin deposition
200	8.1	Thin deposition with strong adherence to the substrate
300	9.7	Thick deposition but weak adherence

The weight of deposited ferrite layers increases with the applied voltage. For low deposition voltage (100 V), the electrophoretic mobility of the particles was probably too low, which usually led to poor deposition rates. This in turn may affect the homogeneity of the deposition. However, applying a higher voltage (300 V), the film exhibited a rough and disordered structure. This is because a higher voltage would cause vigorous movements of particles and renders a rough surface profile of deposit. A slight increase in voltage does promote a faster rate of deposition however it does not guarantee a good adherence of deposition. It has been reported by Ma et al. and Kang et al. for the EPD of PZT powder that EPD at higher voltages is unfavorable for particle packing though the deposition rate can be significantly raised with an increase in the voltage. Figure 4.13 (b) reveals a more uniformly covered film. Therefore, results confirmed that the applied voltage value of 200 V should be used to prepare ferrite films with dense and uniform structure.

4.3.3 Effect of Electrode Separation Distance

When the suspension concentration, deposition time and the applied voltage were kept constant, the effect of electrode separation distance on the deposit weight and the microstructure could be studied. The results and observation were as follows:

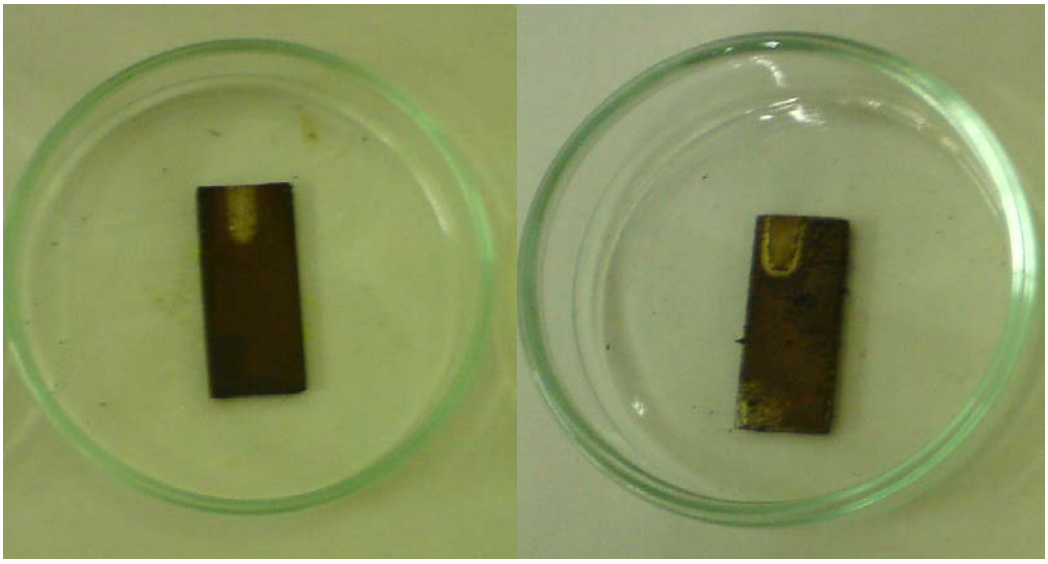

Figure 4.14: Deposited ferrite layers with different electrode separation distance: 10 mm (left); 20 mm (right).

Table 4.7: Observation of ferrite layers deposited via EPD for two different electrodes separation distances

Electrode Separation Distance (mm)	**Weight (mg)**	**Observation**
10	8.6	Thin deposition with strong adherence to the substrate
20	4.0	Very thin and uneven deposition, slow deposition

A bigger electrode separation distance does not promote a thick and dense deposition nor increase in deposition rate. Given the same deposition time, as seen in Table 4.7, the deposit weight decreased to almost one half with an increase in electrode separation distance. The deposition rate with 20 mm electrode separation distance was greatly hampered due to the lower charge strength for particles further away from the electrode. This renders the particles unable to migrate and deposit further than a certain distance.

4.4 Deposition Characterization

Ferrite layers fabricated via EPD with stainless steel electrodes separated by 10 mm with a DC supply of 200 V for one hour deposition time were analyzed using a number of characterization techniques. It is essential to quantitatively describe the structure of the ferrite layers as well as its composition.

4.4.1 Field Emission Scanning Electron Microscope (FE-SEM)

Field emission scanning electron microscope (FE-SEM) was used to examine the surface morphology of the ferrite layers deposited at different magnifications. Figures 4.15 – 4.20 show the FE-SEM photographs of nickel zinc ferrite and magnesium copper zinc ferrite films formed on stainless steel electrode.

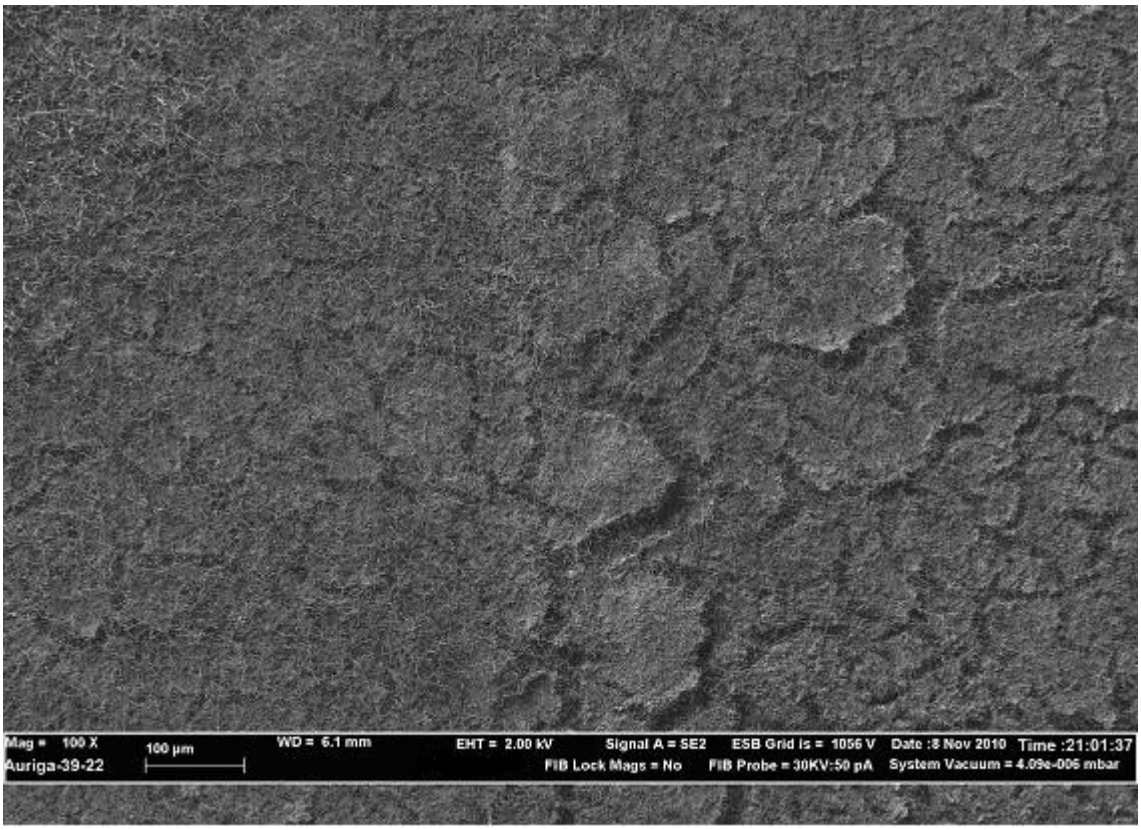

Figure 4.15: FE-SEM image of the sintered nickel zinc ferrite film (100X Magnification).

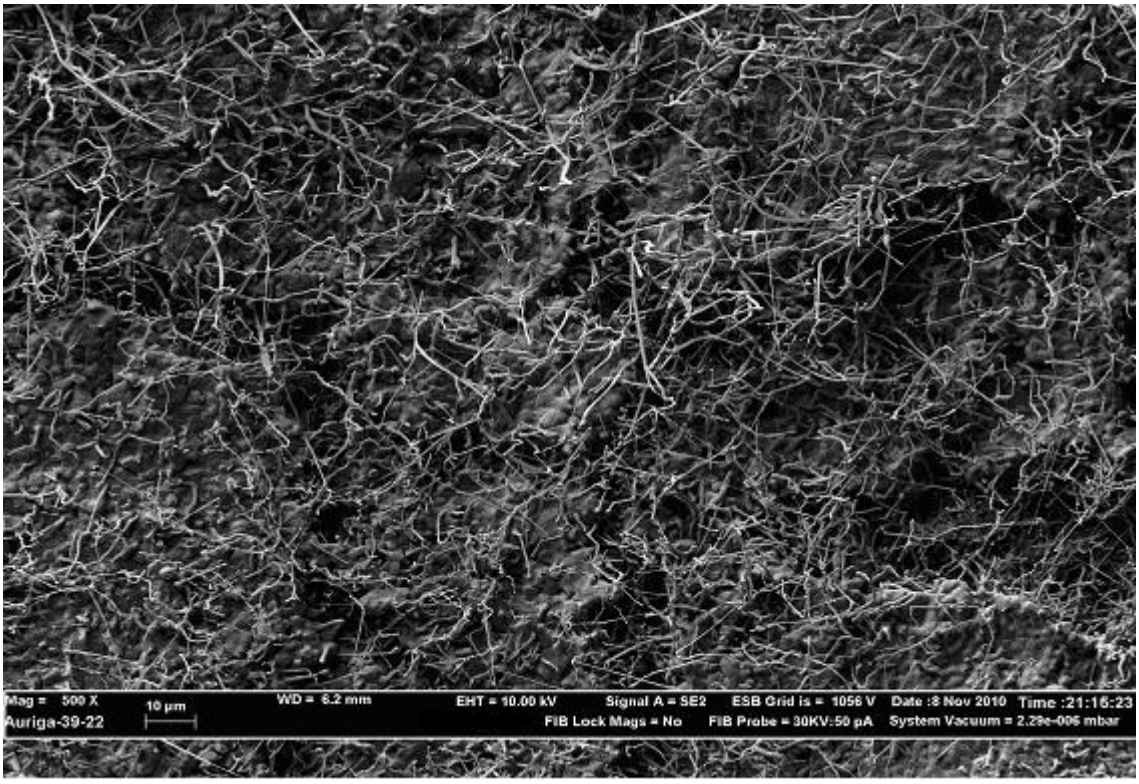

Figure 4.16: FE-SEM image of the sintered nickel zinc ferrite film (500X Magnification).

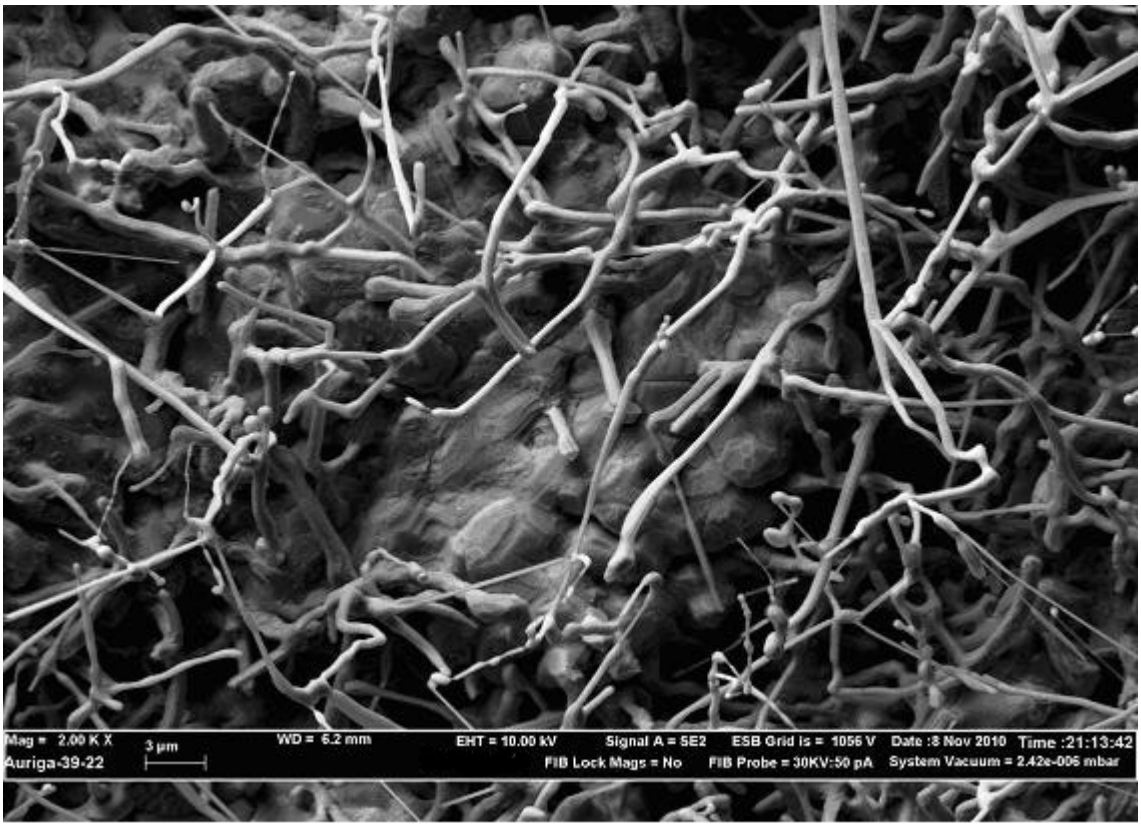

Figure 4.17: FE-SEM image of the sintered nickel zinc ferrite film (2000X Magnification).

FE-SEM images of the surface morphology of the nickel zinc ferrite layer are shown in Figures 4.15 – 4.17. In general, the film is homogeneous and continuous. As seen from Figure 4.15, cracks are detected in the ferrite layer. The non-uniformities are caused by the post deposition drying process and further optimization needs to be done to get uniform deposition at nanoscales. Needle-like structure (diameters of ~3.75 μm and of length up to 25 μm) can be seen on top of the surface of the ferrite layer. The long thin shape as shown in Figure 4.17 can be seen throughout the surface of elecrtode due to the formation of repeated thin layers of ferrite.

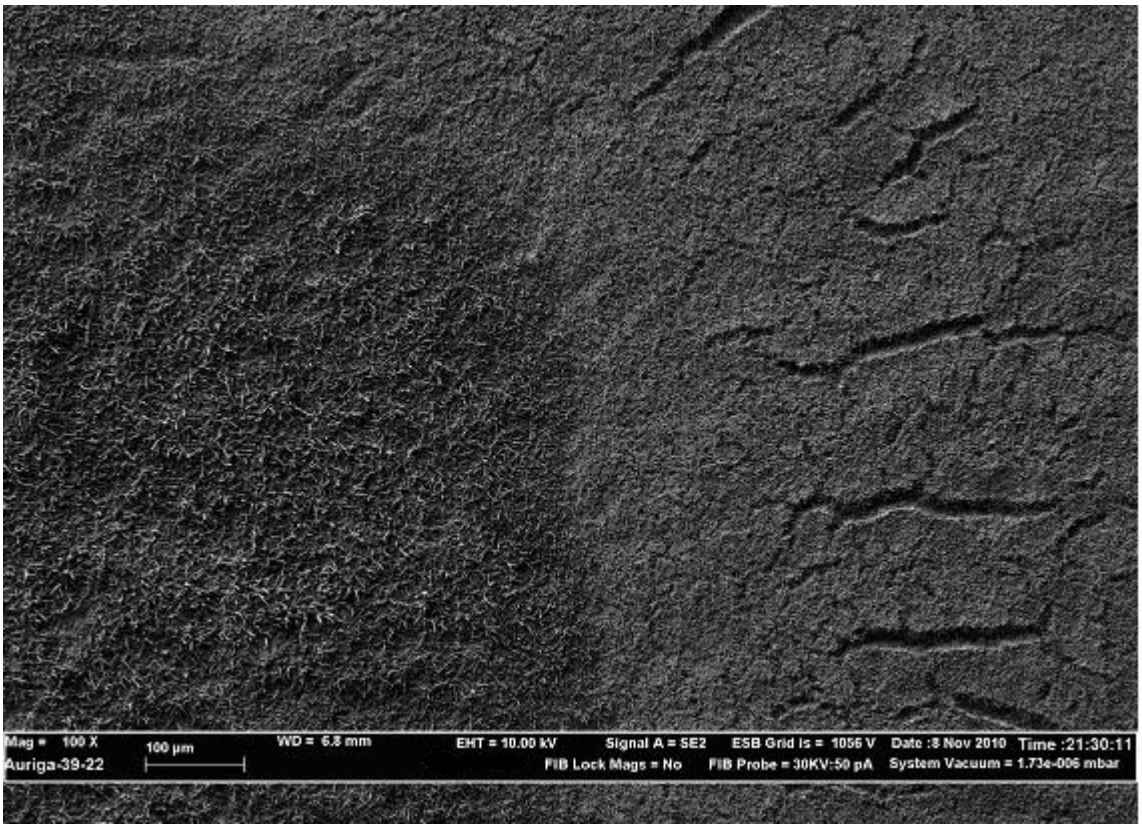

Figure 4.18: FE-SEM image of the sintered magnesium copper zinc ferrite film (100X Magnification).

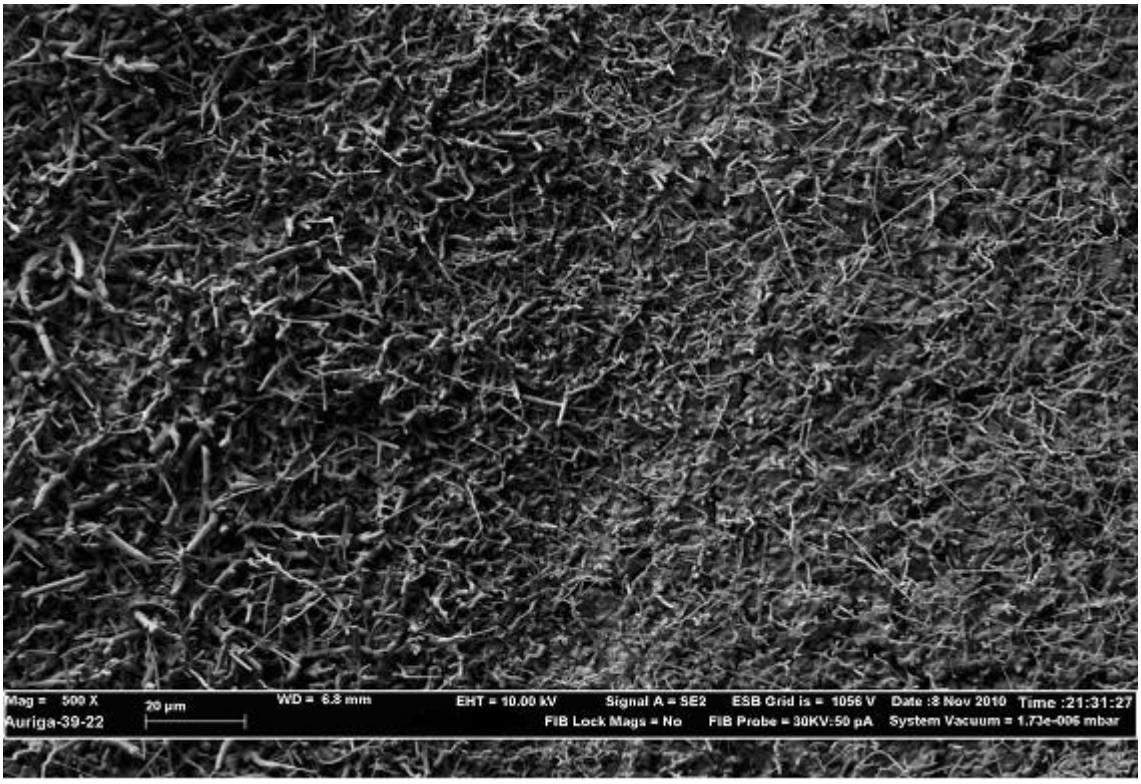

Figure 4.19: FE-SEM image of the sintered magnesium copper zinc ferrite film (500X Magnification).

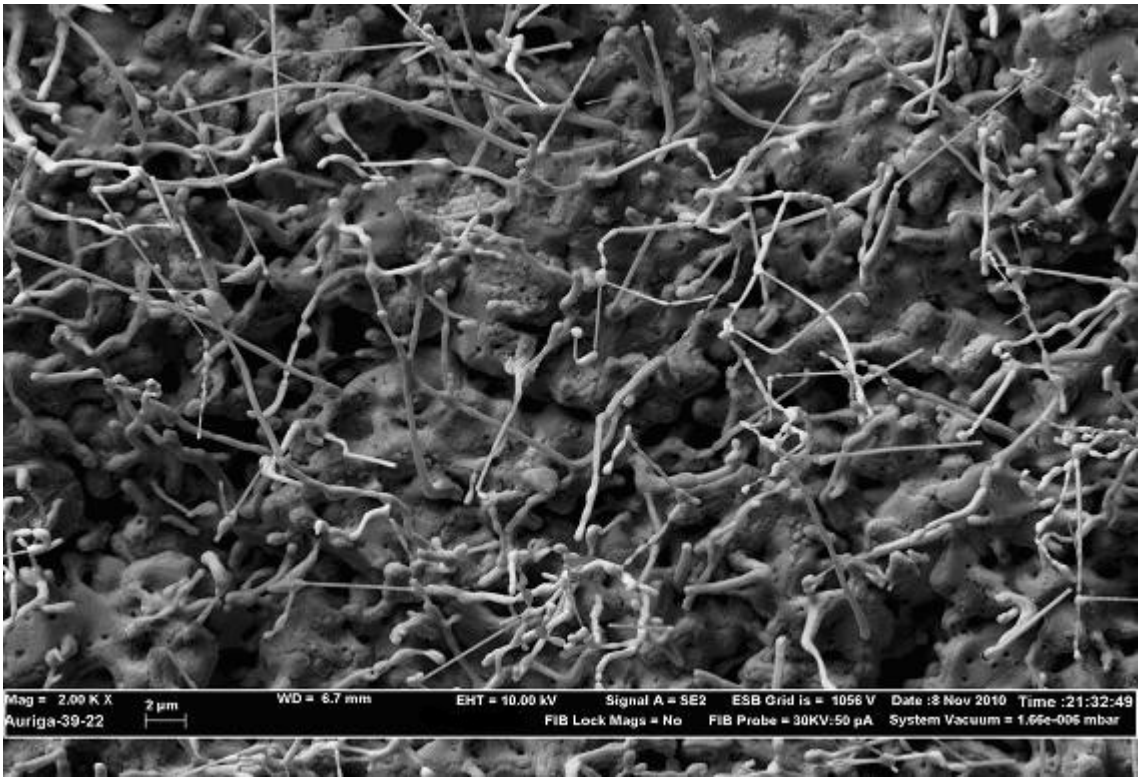

Figure 4.20: FE-SEM image of the sintered magnesium copper zinc ferrite film (2000X Magnification).

Figures 4.18 – 4.20 show the FE-SEM images of the surface morphology of the magnesium copper zinc ferrite layer, deposited on the cathode. It is noticeable that cracks occurred for the deposited magnesium copper zinc ferrite layer as shown in Figure 4.18. It indicates that ferrite layer was not fully closed packing with some visible defects. The ferrite layer deposited is similar to the surface strucure of nickel zinc ferrite layer which is in the form of needle-like shape (diameters of ~3.75 μm and of length up to 12 μm).

4.4.2 Energy Dispersive X-ray Spectroscopy (EDX)

Characterizations of the compositions of ferrite layers prepared in this study were carried out using Energy Dispersive X-ray Spectrometer (EDX). Figure 4.21 and 4.22 show EDX spectra of samples deposited.

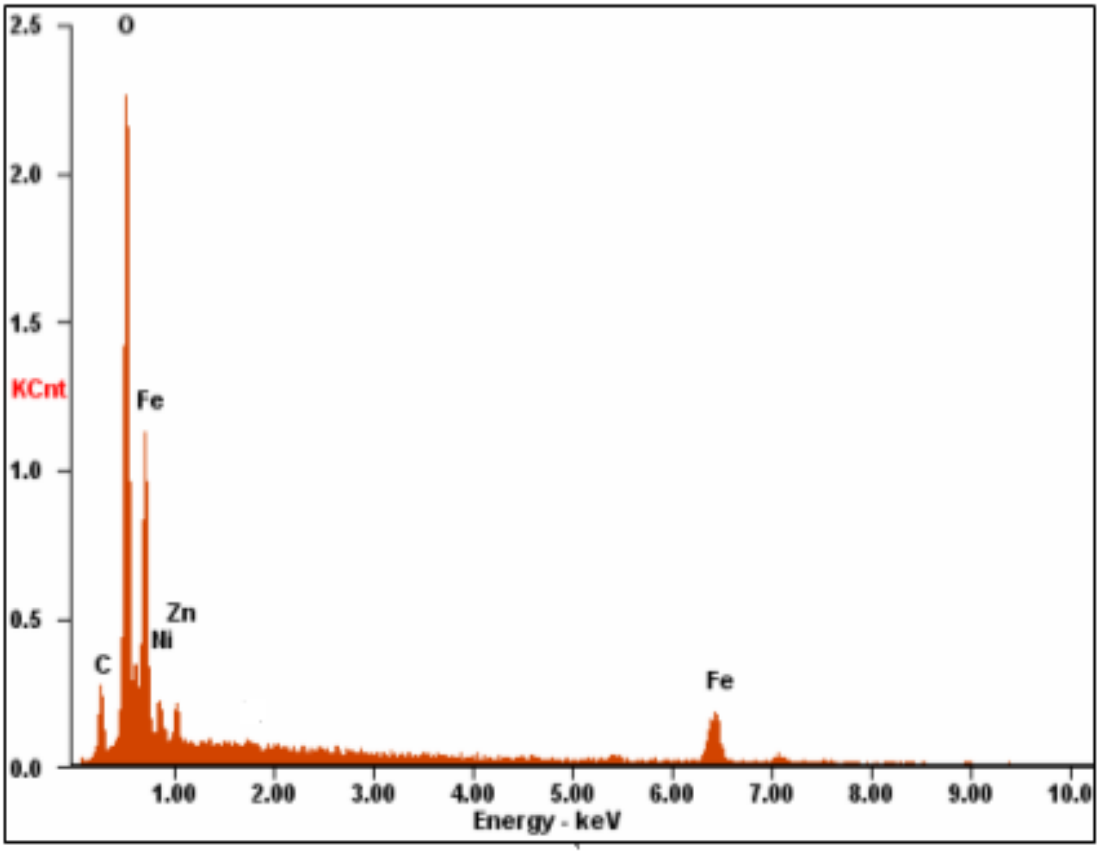

Figure 4.21: EDX spectrum of nickel zinc ferrite layer deposited on stainless steel cathode.

Figure 4.21 shows the spectra of the sintered nickel zinc ferrite layer deposited on stainless steel cathode. It is observed that only a small trace of nickel and zinc matrix can be identified. Elements of iron and oxygen confirming ferrite layer is present in the deposition.

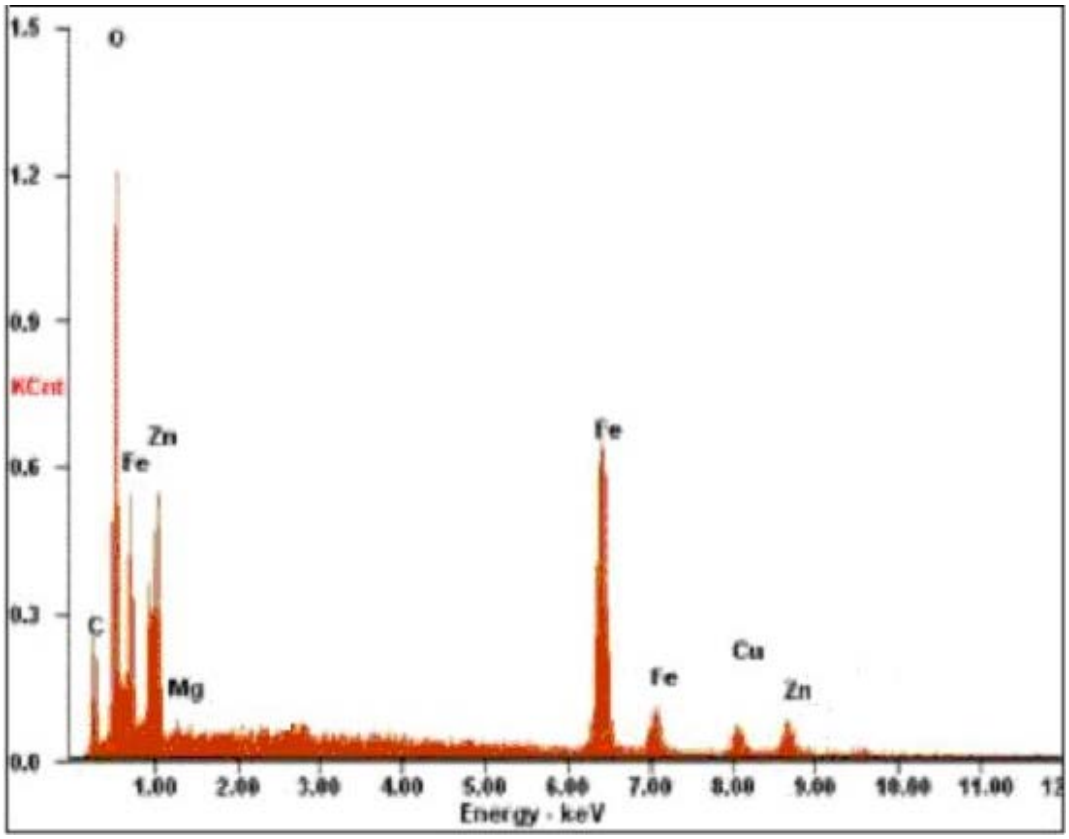

Figure 4.22: EDX spectrum of magnesium copper zinc ferrite layer deposited on stainless steel cathode.

Figure 4.22 shows the spectra of the sintered magnesium copper zinc ferrite layer deposited on stainless steel cathode. It is observed that only a small trace of magnesium, copper and zinc matrix can be identified. Similarly, elements of iron and oxygen confirming ferrite layer is present in the deposition.

4.4.3 X-ray Diffraction (XRD)

The deposited ferrite layers were subjected to phase analysis by employing X-ray diffractometer, which was equipped with graphite monochromator, a mirror at a fixed incidence angle of 1.5°and CuKα as radiation source (λ = 1.54184 Å). Figure 4.23 and Figure 4.24 show the X-ray diffraction patterns of the nickel zinc ferrite and magnesium copper zinc ferrite layer.

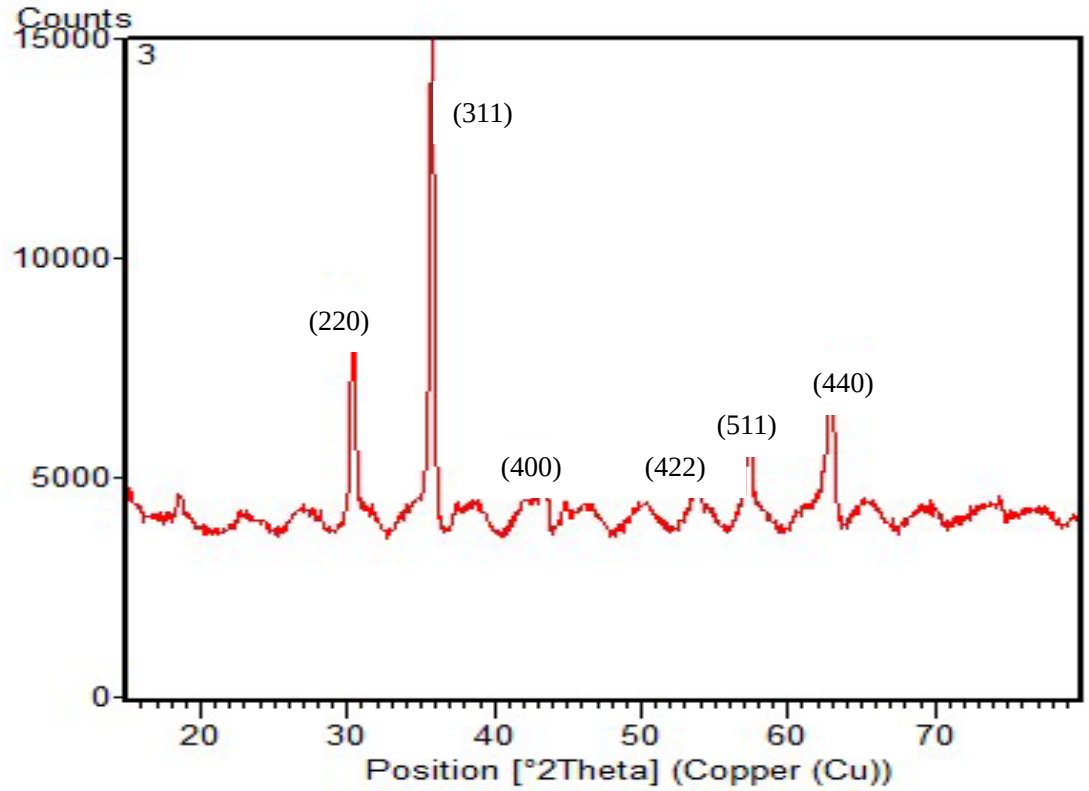

Figure 4.23: XRD pattern of sintered nickel zinc ferrite layer.

Figure 4.23 shows the X-ray diffraction (XRD) pattern of sintered nickel zinc ferrite layer. The ferrite film is polycrystalline as seen from the well-defined peaks in the pattern. Also, all the basic components of $Ni_{0.5}Zn_{0.5}Fe_2O_4$ powder in various oxidation states were detected which is in accordance with PDF#54-0964 from the International Centre for Diffraction Data (ICDD) PDF-4. It can be concluded from the

analysis that a ferrite film is present and that it retained the spinel structure of the ferrite powder produced by the water-in-oil microemulsion method. Organic impurities from additives such as the dispersant and the charging agent did decompose during sintering at 1000 °C in the presence of argon gas.

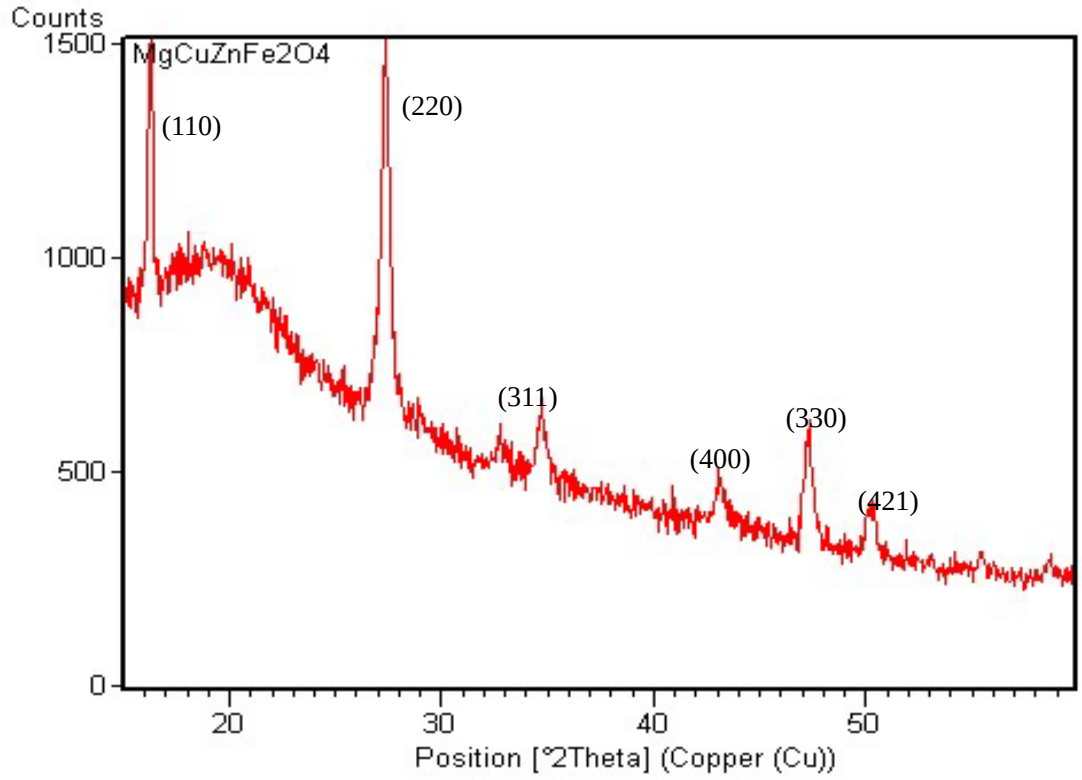

Figure 4.24: XRD pattern of sintered magnesium copper zinc ferrite layer.

Figure 4.24 shows the XRD patterns of calcined magnesium copper zinc ferrite nanoparticles. Magnesium copper zinc ferrite is polycrystalline as seen from the well-defined peaks in the pattern. All the basic components of $Mg_{0.09}Cu_{0.34}Zn_{0.57}Fe_2O_4$ powder in various oxidation states were detected in accordance with PDF#51-0384 from the International Centre for Diffraction Data (ICDD).

4.4.4 Atomic Force Microscope (AFM) and Magnetic Force Microscope (MFM)

The use of atomic and magnetic force microscopies (AFM and MFM respectively) have been employed to differentiate between magnetic and non magnetic phases in materials. In MFM, the magnetic fields adjacent to a sample are detected with sub-micron resolution, by scanning a magnetic probe over the surface and recording the changes in its phase or resonant frequency (Wittborn, 2000). Figures 4.25 – 4.28 show the AFM/MFM topography of the deposited ferrite layer. The ferrite films were scanned over a 20.0 μm x 20.0 μm area.

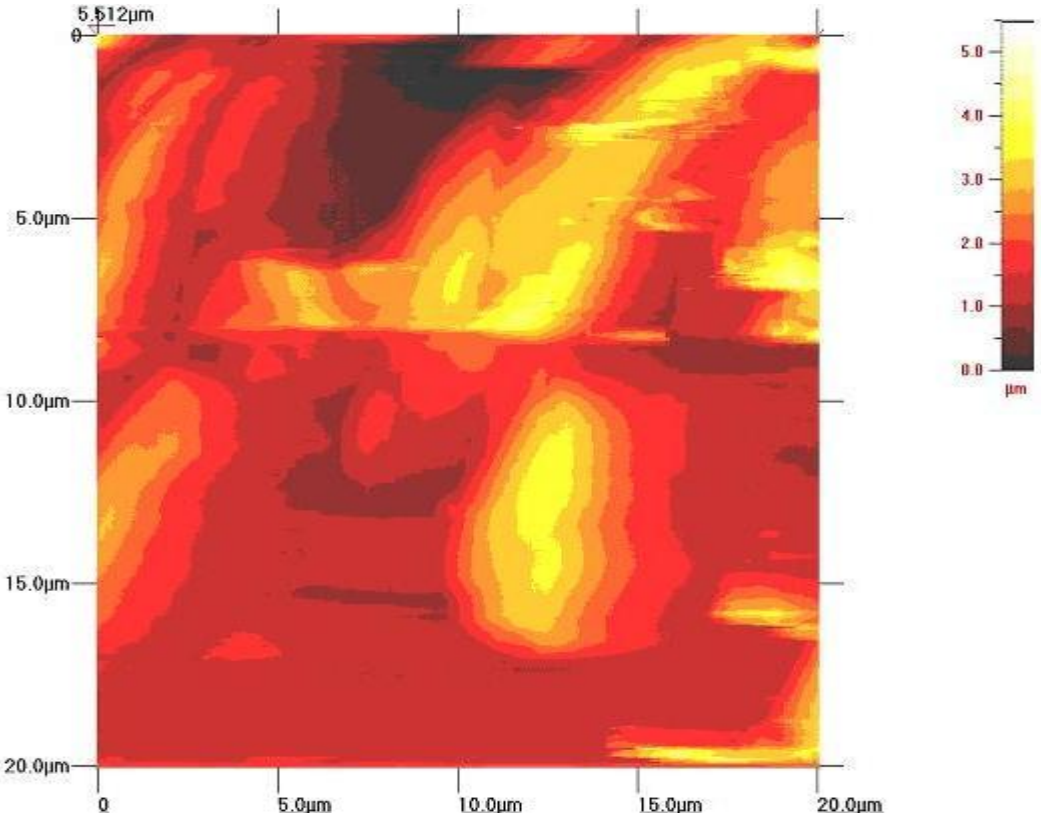

Figure 4.25: AFM image of sintered nickel zinc ferrite layer.

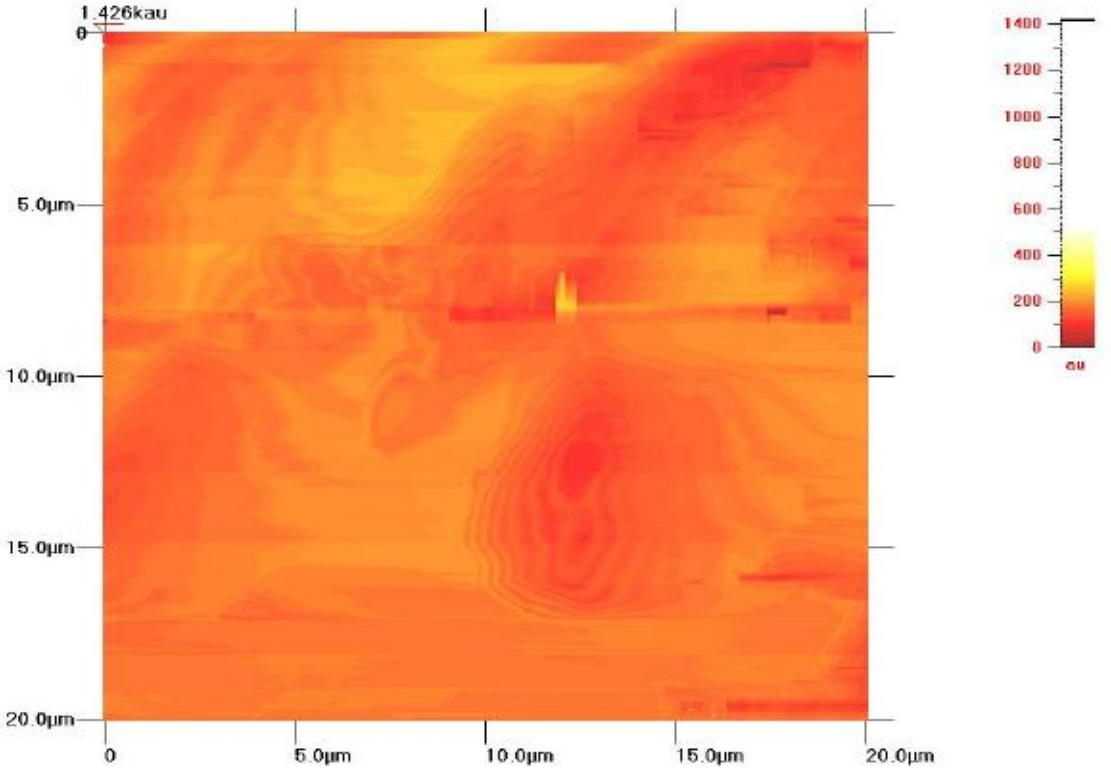

Figure 4.26: MFM image of sintered nickel zinc ferrite layer.

The regions of bright contrast in AFM topology image or the regions of dark contrast in MFM image indicated magnetic domains in the ferrite film. The magnetic domains have irregular shape and they extend over the whole scan area. As shown in Figure 4.26, different magnetic patterns are observed as a result of the fine domain structure in the deposited nickel zinc ferrite layer. The contrast of the dark and bright regions indicated the domain walls of the needle-like structure in ferrite film.

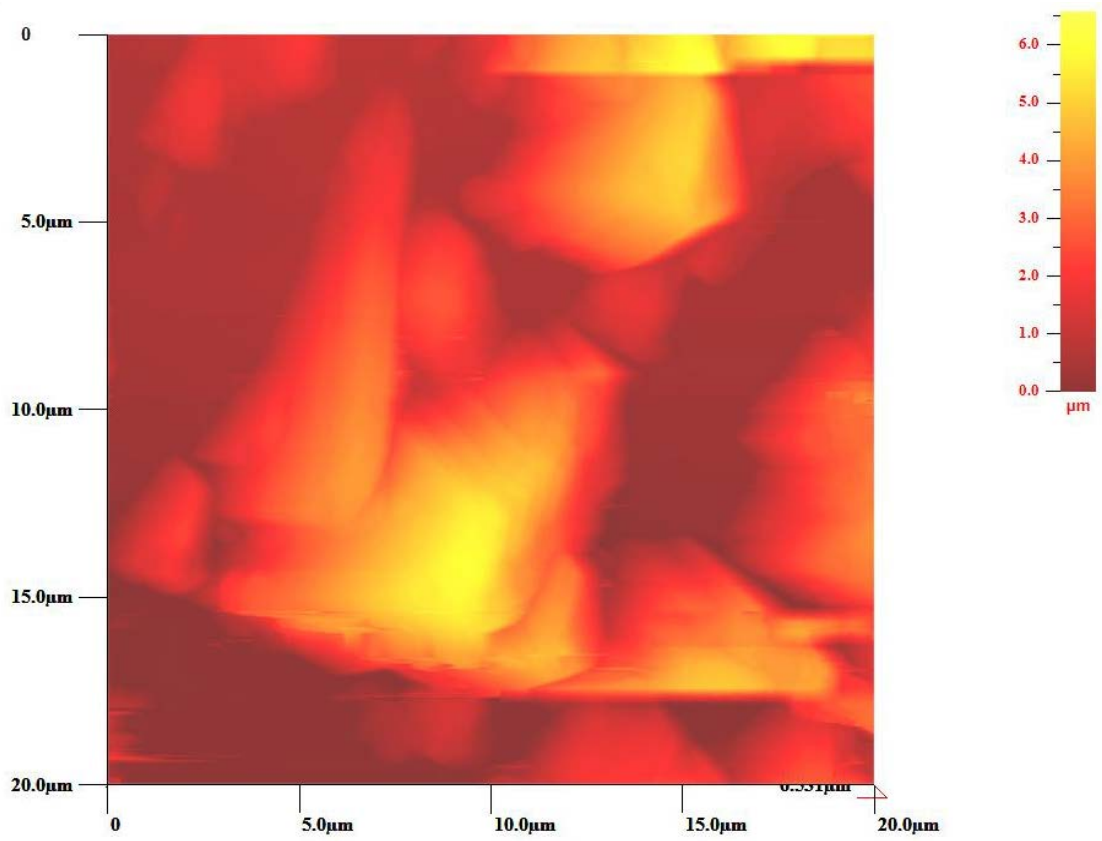

Figure 4.27: AFM image of sintered magnesium copper zinc ferrite layer.

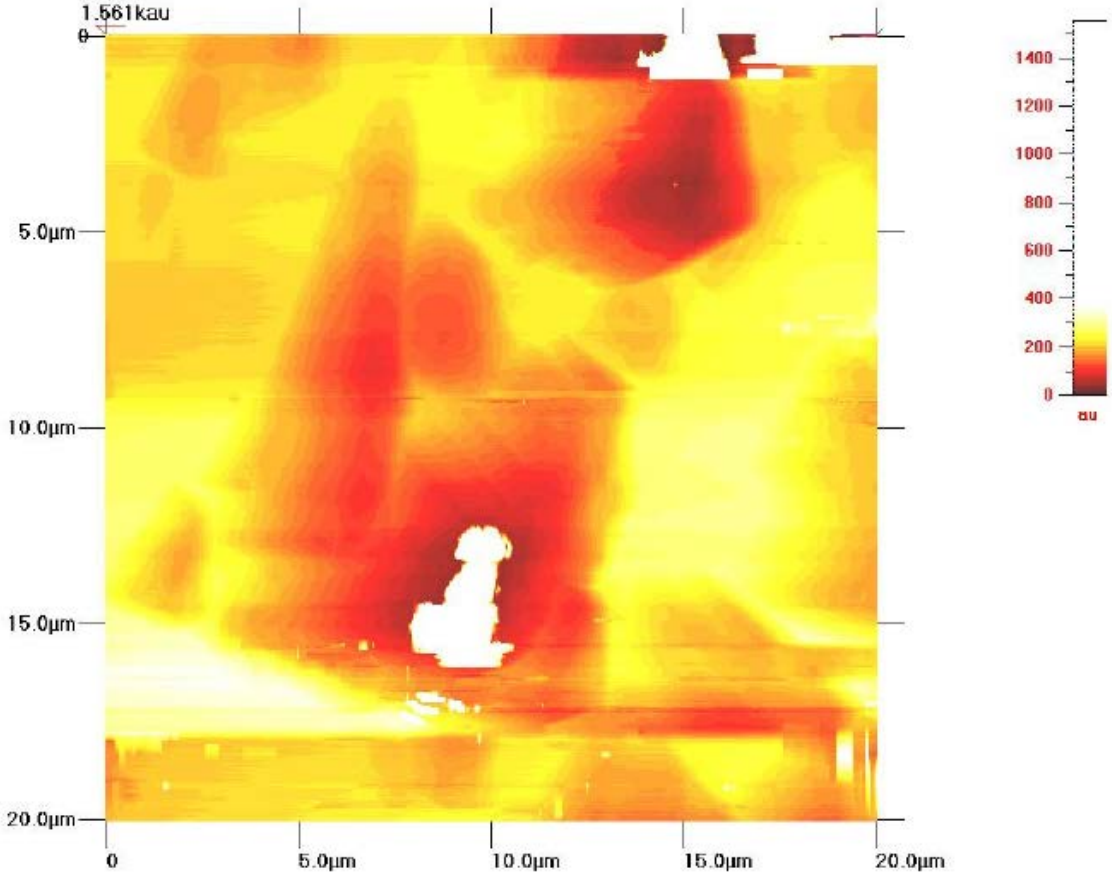

Figure 4.28: MFM image of sintered magnesium copper zinc ferrite layer.

Similarly, the regions of bright contrast in AFM topology image or the regions of dark contrast in MFM image indicated magnetic domains in the magnesium copper zinc ferrite film. Figure 4.28 shows sharper image with better lateral resolution if compared with magnetic pattern observed in nickel zinc ferrite layer. However, the white spot near the fringing field of magnetic domains in Figure 4.28 indicated that the magnetic structure was seriously perturbed. This is because the deposition is too rough for the cantilever to reach through using scanning probe microscope. It is important to note that continuous film with smooth surface is preferred for better imaging.

CHAPTER 5

CONCLUSION AND RECOMMENDATIONS

5.1 CONCLUSION

Nanostructured nickel zinc ferrite and magnesium copper zinc ferrite powder have prepared by water-in-oil microemulsion technique. Transmission electron micrographs show agglomerated nanoparticles with an average crystallite size of 26.6 nm for magnesium copper zinc ferrite and 22.7 nm for nickel zinc ferrite. Ferrite powders prepared exhibit soft ferromagnetic bahaviour with a low coervicity value.

It was found that the suspension of ethanol with Phosphate Ester (PE) as charging agent, PVB as binder and PEI as dispersant is suitable for use in EPD. The highest zeta potential (34.4 mV) was recorded from the suspension of 0.1 wt% ferrite, 99.9 wt% ethanol with 4 wt% PE, 1 wt% PVB and 1 wt% PEI. Correlation between pH, conductivity and zeta potential of the suspension were clearly demonstrated in determining the suspension stability. The dissociation of PE results in liberation of hydronium ions (H+) which mobilize the ferrite particles. This gives rise to the zeta potential and at the same time decreases the pH of the suspension. Proper manipulation of pH and zeta potential could result in better suspension stability and subsequently a good deposition layer can be produced. In addition, the effect of solid concentration by varying the weight percentage of ferrite powder in the suspension shows that higher solid concentration lead to lower suspension stability and lower electrophoretic mobility.

Electrophoretic deposition process is a versatile technique for producing ferrite layers of a wide range of composition at a relatively low temperature and a high deposition rate. Ferrite layers could be deposited via cathodic electrophoretic deposition. EPD parameters such as applied voltage, electrode materials and electrode separation distance influenced on the deposit weight, morphology and microstructure of the ferrite layers. A dense ferrite layer with good adhesion to the substrate could be obtained by using stainless steel electrodes with electrodes separation distance of 10 mm and DC supply of 200 V for one hour deposition time.

The FE-SEM images for both sintered nickel zinc ferrite and magnesium copper zinc ferrite layers exhibited a homogeneous film composed of needle-like crystal structure. EDX and XRD analysis confirmed the composition of the ferrite layers formed. Magnetic domains of the ferrite films were detected using scanning probe microscope. The success of the EPD of ferrite nanoparticles depends on the optimization of the suspension and system parameters.

5.2 RECOMMENDATIONS

Suspension medium and the additives play a crucial role for electrophoretic forming. Formation of fine and more uniform ferrite powders should be used to obtain a well-stabilized colloidal suspension. In order to form a stable suspension to be used for electrophoretic deposition, a solvent capable of carrying enough current to facilitate electrophoresis must be employed in the apparatus.

Sintering process is an important procedure to further densify the deposit and eliminate porosity. Consolidation of coating with the substrate was enhanced by sintering the deposit at 1000 ºC. Sintering had to be carried out in inert conditions as the stainless steel electrode is highly susceptible to oxidation at high temperatures. Inert gases like argon and nitrogen are required to be used in tube furnace.

Suitable experiments should be conducted on the ferrite deposit to determine the magnetic properties. The working frequency of the ferrite layers can be further studied by using impedance analyzer. It is crucial to examine the quality of the ferrite deposit for further development in the electronics industry.

REFERENCES

Ang, B. C. and Yaacob, I. I. (2007). Synthesis and characterization of magnetic iron oxide nanoparticles via w/o microemulsion and Massart's procedure. *J. Mater. Process. Technol.* **191**, 235-237.

Arriagada, F. J. and Osseo-Asare, K. (1999). Synthesis of nanosize silica in a nonionic water-in-oil microemulsion: effects of the water/surfactant molar ratio and ammonia concentration. *J. Colloid & Interf. Sci.* **211**, 210-220.

Berkowitz, A. E., Shuele, W. J. and Flanders, P. J. (1968). Interference of crystallite size on the magnetic properties of acicular γ-Fe_2O_3 particles. *J. Appl. Phys.* **39**, 1261-1263.

Besra, L. and Liu, M. (2007). A review on fundamentals and applications of electrophoretic deposition (EPD). *J. Progress in Mater. Sci*. **52**, 1-61.

Boccaccini, A. R., Roether, J. A., Thomas, B. J. C., Shaffer, M. S. C., Chavez, E., Stoll, E. and Minay, E. J. (2006). The electrophoretic deposition of inorganic nanoscaled materials – a review. *J. Ceram. Soc. Jpn*. **114** (1), 1-14.

Burrieaci, N., Nannetti, A., Petrera, M., Pizzini, S., Benedek, G. and Biasutto, L. (1977). Comparison of structural and magnetic properties of Zn/Mn ferrites prepared by wet-chemical and ceramic methods. *J. Mater. Chem*. **2**, 241-251.

Callister, J. W. D. (2003). Material Science and Engineering: An Introduction, 6th Ed. New York: John Wiley & Sons Inc.

Caragheorgheopol, A., Caldararu, H., Vasilescu, M., Khan, A., Angelescu, D., Zilkova, N. and Cejka, J. (2004). Structural characterization of micellar aggregates in sodium dodecyl sulfate/ aluminum nitrate/ urea/ water system in the synthesis of mesoporous alumina. *J. Phys.Chem.* **108** (23), 7735-7743.

Chen, C. Y., Chen, S. Y. and Liu, D. M. (1999). Electrophoretic deposition forming of porous alumina membranes. *Acta Mater*. **47** (9), 2717–2726.

Ciou, S. J., Fung, K. Z. and Chiang, K. W. (2007). The mathematical expression for kinetics of electrophoretic deposition and the effects of applied voltage. *J. Power Sources*. **172**, 358–362.

Corni, I., Ryan, M. P. A. and Boccaccini A. R. (2008). Electrophoretic deposition: From traditional ceramics to nanotechnology. *J. Eur. Ceram. Soc*. **28**, 1353–1367.

Daliya, S. M. and Juang, E. S. (2007). An overview of the structure and magnetism of spinel ferrite nanoparticles and their synthesis in microemulsions. *Chem Eng J*. **129**, 51-65.

Doungdaw, S., Uchikoshi, T., Noguchi, Y., Eamchotchawalit, C. and Sakka, Y. (2005). Electrophoretic deposition of lead zirconate titanate (PZT) powder from ethanol suspension prepared with phosphate ester. *Sci. Technol. Adv. Mater*. **6**, 927–932.

Guo, D., Cai, K, Li, L., Huang, Y., Gui, Z. and Zhu H. (2000). Electrodeposition of diamond-like amorphous carbon films on Si from n,n-dimethylformamide. *Chem. Phys. Lett.* **329** (5-6), 346-350.

Hamaker, H. C. (1940). Formation of a deposit by electrophoresis. *Trans. Faraday Soc.* **36**, 279-287.

Hassan, R. S., Viart, N., Ulhaq-Bouillet, C., Loison, J. L., Versini, G., Vola, J. P. And Cregut O. (2007). Structural properties of cobalt ferrite thin films deposited by pulsed laser deposition: Effect of the reactive atmosphere. *Thin Solid Films.* **515**, 2943-2948.

Hashi, S., Takada, N., Nishimura, K., Sakurada, O., Yanase, S., Okazaki, Y, and Inoue, M. (2006). The fabrication technique for over 10-μm-thick ferrite particulate film at room temperature. *IEEE Trans. on Magn.* **41** (10), 3487-3489.

Hashi, S., Tokunaga, Y., Nishimura, K., Yanase, S., Okazaki, Y, Sakurada, O., Nishimura, K. and Inoue, M. (2004). Magnetic properties of electrophoretic deposited ferrite particulate films. *IEEE Trans. on Magn*. **44** (104), 2796-2798.

Holmberg, K. (2004). Surfactant-templated nanomaterials synthesis. *J. Colloid & Interf. Sci*. **274**, 335-364.

Jang, S. P. and Choi, S. (2004). Role of brownian motion in the enhanced thermal conductivity of nanofluids. *Appl. Phys. Lett.* **84**, 4316-4318.

Jiles, D. C. (2003). Recent advances and future directions in magnetic materials. *Acta Mater.* **51**, 5907-5939.

Kang, N., Gong, W., Liu, J. and Li, J. F. (2004). Fabrication of PZT thick films on silicon wafer by powder electrophoretic deposition. *J. Ceram. Soc. Jpn.* **112** (Suppl. 1), S506-S509 [PacRim Special Issue].

Koay, M. H. (2004). *Influence of Composition on the Electromagnetic Properties of Mg-Cu-Zn Ferrites*. Master Thesis, University of Malaya, Kuala Lumpur.

Kurinec, S. K., Okeke, N., Gupta, S. K., Zhang, H. and Xiao, T. D. (2006). Synthesis and electrophoretic deposition of magnetic nickel ferrite nanoparticles. *J. Mater. Sci.* **41**, 8181-8185.

Kurinec, S. K. and Sluzky, E. (1996). Fabrication of ultra-high-resolution three-color phosphor screens. *J. Soc. Info. Displays.* **4** (4), 371-373.

Kuscer, D. and Kosec, M. (2010). $0.65Pb(Mg_{1/3}Nb_{2/3})O_3$-$0.35PbTiO_3$ thick films prepared by electrophoretic deposition from an ethanol-based suspension. *J. Eur. Ceram. Soc.* **30**, 1437-1444.

Liu, X., Wang, J., Gan, L. M., Ng, S. C. and Ding, J. (1998). An ultrafine barium ferrite powder of high coercivity from water-in-oil microemulsion. *J. Magn. Magn. Mater.* **184**, 344-354.

Ma, J. and Cheng, W. (2002). Deposition and packing study of sub-micron PZT ceramics using electrophoretic deposition. *Mater. Lett.* **56**, 721-727.

Mehrali, M., Wakily, H. and Metselaar, I. H. S. C. (2011). Residual stress and mechanical properties of Al_2O_3/ZrO_2 functionally graded material prepared by EPD from 2-butanone based suspension. *Adv in Applied Ceram.* **110**, 35-40.

Ng, B. S. (2008). *The Influence of Different Amount of Triton X-100 on the Properties of Mg-Cu-Zn Ferrite*. Degree Dissertation, University of Malaya, Kuala Lumpur.

Nordiana, N. (2010). *The Effects of Particles Size and Zeta Potential on Properties of Mg-Cu-Zn Ferrite Prepared by Electrophoretic Deposition*. Degree Dissertation, University of Malaya, Kuala Lumpur.

Ong, K. Y. (2007). *Influence of Surfactant Concentration on Sintering Behavior of Co-precipitation Ferrites*. Degree Dissertation, University of Malaya, Kuala Lumpur.

Ogata, N., Van Tassel, J. and Randall, C. A. (2001). Electrode formation by electrophoretic deposition of nanopowders. *Mater. Lett.* **49**, 7-14.

Palmqvist, A. E. C. (2003). Synthesis of ordered mesoporous materials using surfactant liquid crystals or micellar solutions. *Curr. Opin. Colloid Interf. Sci*. **8**, 145-155.

Pileni, M. P. (1993). Role of soft colloidal templates in the control of size and shape of inorganic nanocrystals. *Nature Mater.* **2**, 145-150.

Powers, R. W. (1975). The electrophoretic forming of beta-alumina ceramic. *J. Electrochem. Soc.* **122**, 490-500.

Raj, P. M., Muthana, P., Xiao, T. D., Wan, L., Balaraman, D., Abothu, I. R., Bhattacharya, S., Swaminathan, M. and Tummala, R. (2005). Magnetic nanocomposites for organic compatible miniaturized antennas and inductors. *IEEE Conf Adv Packaging Mater.* **16**, 272-275.

Ravinder, D., Kumar, K. V. and Reddy, A. V. R. (2003). Preparation and magnetic properties of Ni-Zn ferrite thin films. *Mater. Lett.* **57**, 4162-4164.

Reed, J. S. (1995). Principles of Ceramics Processing, 2nd Ed. New York: John Wiley & Sons, Inc.

Rivas, J., Quintela, M. L., Perez, J. L. and Liz, L. (1993). First steps towards tailoring fine and ultrafine iron particles using microemulsions. *IEEE Trans. Magn*. **29**, 2655-2657.

Sahara, S. and Yamaguchi T. (1969). Dissociation and crystal distortion of copper ferrite. *J. Jpn. Soc. of Powder & Powder Metallurgy*. **15**, 445-448.

Sarkar, P. and Nicholson, P. S. (1996). Electrophoretic deposition (EPD): mechanism, kinetics and application to ceramics. *J. Am. Ceram. Soc.* **79**, 1987-2002.

Sasaki, K. Y. and Talbot, J. B. (1999). Deposition of powder phosphors for information displays. *Adv. Mat*er. **11** (2), 91-105.

Sato, N., Kawachi, M., Noto, K., Yoshimoto, N. and Yoshizawa, M. (2001). Effect of particle size reduction on crack formation in electrophoretically deposited YBCO films. *J. Phys. Chem*. **22**, 357-360.

Shahane, G. S., Kumar, A., Arora, M., Pant, R. P., and Lal, K. (2009). Synthesis and characterization of Ni-Zn ferrite nanoparticles. *J. Magn. Magn. Mater*. **322**, 1015-1019.

Stappers, L., Zhang, L., Van der Biest, O. and Fransaer, J. (2008). The effect of electrolyte conductivity on electrophoretic deposition. *J. Electrochem. Soc*. **328**, 436-446.

Talbot, J. B., Sluzky, E. and Kurinec, S. K. (2004). Electrophoretic deposition of monochrome and color phosphor screens for information displays. *J. Mater. Sci.* **39** (3), 771-778.

Thakur, S., Katyal, S. C. and Singh, M. (2009). Structural and magnetic properties of nano nickel-zinc ferrite synthesized by reverse micelle technique. *J. Magn. Magn. Mater*. **321**, 1-7.

Vandeperre, L., Van der Biest, O. and Clegg, W. J. (1997). Silicon carbide laminates with carbon interlayers by electrophoretic deposition. *Key Eng. Mater. (Ceram. & Metal Matrix Composites).* **127-131**, 567-574.

Van der Biest, O. O. and Vanderperre, L. J. (1999). Electrophoretic deposition of materials. *Annu. Rev. Mater. Sci.* **29**, 237-252.

Verma, A., Alam, M. I., Chatterjee, R., Goel, T. C. and Mendiratta, R. G. (2006). Development of a new soft ferrite core for power applications. *J. Magn. Magn. Mater.* **300,** 500-505.

Washburn, C. Brown, D., Cabacungan, J., Venkataraman, J and Kurinec, S. K. (2005). Materials, integration and technology for monolithic instruments. *Mater. Research Soc. Symposium Proceeding.* **869**, 157.

Weise, N. L. (1985). SME Mineral Processing Handbook: Vol. 1. New York: Society of Mining Engineers.

Wittborn, J. (2000). *Nanoscale Studies of Functional Materials using Scanning Probe Microscopy*. Doctoral Thesis, Royal Institute of Technology, Stockholm, Sweden.

Zahi, S., Hashim, M. and Daud, A. R. (2007). Synthesis, magnetic properties and microstructure of Ni-Zn ferrite by sol-gel technique. *J. Magn. Magn. Mater.* **308**, 177-182.

Zarbov, M., Schuster, I. and Gal-Or, L. (2004). Methodology for selection of charging agents for electrophoretic deposition of ceramic particles. *J. Mater. Sci*. **39**, 813– 817.

Zhitomirsky, I. and Petric, A. (2000). Electrophoretic deposition of ceramic materials for fuel cell applications. *J. Eur. Ceram. Soc.* **20**, 2055-2061.

INTERNET REFERENCES

1. (URL-http://www.ifp.tuwien.ac.at/institut/lva/skripten/), 7/9/2009a.
2. (URL-http://www.tf.uni-kiel.de/matwis/amat/def_en/kap_2/basics/b2_1_6.html), 7/9/2009b.
3. (URL-http://www.tdk.co.jp/tefe02/e181.pdf), 2/10/2009.
4. (URL-http://www.made-in-china.com/showroom/vivianzhang/product-detailsJxnoHRXsmMk/China-Polyvinyl-Butyral-PVB-Resin.html), 9/10/2009a.
5. (URL-http://www4.ncsu.edu/~hubbe/PEI.htm), 9/10/2009b.
6. (URL-http://msel.nist.gov/Nanotube2/Practice%20Guide_Section%202_TGA.pdf), 10/10/2009.
7. (URL-http://www.malvern.com/LabEng/products/Mastersizer/ms2000/mastersizer2000.htm), 11/10/2009a).
8. (URL-http://en.wikipedia.org/wiki/Energy_dispersive_X-ray_spectroscopy), 11/10/2009b.
9. (URL-http://www.malvern.com/labeng/products/zetasizer/zetasizer.htm), 11/10/2009c.
10. (URL-http://www.aandd.jp/products/test_measuring/sv10/sv10.html), 11/01/2011.

APPENDIX

Suspension Calculation

Density of ethanol = 0.789 g/cm^3

Density of tri-n-butyl phosphate (PE) = 0.979 g/cm^3

Density of polyethyleneimine (PEI) = 1.07 g/cm^3

99.9 wt% ethanol + 0.1 wt% ferrite + 4 wt% PE + 1 wt% PEI + 1 wt% PVB

Ethanol = 80 ml

Density = mass/volume

0.789 = x g / 80 cm^3

x = 63.12 g

Ferrite = (0.1/99.9 x 63.12)

= 0.0632 g / 63.2 mg

PE = 0.0632 x 4%

= 2.527 x 10^{-3} g

= mass/0.979

= 2.582 x 10^{-3} ml

= 2.582 μl

PEI = 0.0632 x 1%

= 6.32×10^{-4} g

= mass/1.07

= 0.591×10^{-3} ml

= 0.591 μl

PVB = 0.0632 x 1%

= 0.632×10^{-3} g / 0.632 mg

PUBLICATIONS

Hee, A. C., Metselaar, I. H. S. C., Johan, M. R. and Mehrali, M. (2012). Preparation of nickel zinc ferrite by electrophoretic deposition. *J. Electrochem. Soc.* **159 (1)**, E18-E22.

Hee, A. C., Metselaar, I. H. S. C. and Johan, M. R. (2011). Preparation of nickel zinc ferrite thin film by electrophoretic deposition, *Proceedings: Asia International Magnetics Conference, InterMag 2011,* Taiwan: Taipei, pp. 128.

Johan, M. R., Suan, M. S., Hawari, N. and Hee, A. C. (2011). Annealing effects on the properties of Copper Oxide Thin Films by prepared by chemical deposition. *Inter. J. Electrochem. Sci.* **6**, 6094-6104.